2011-04-12

Strain Monitoring of Carbon Fiber Composite with Embedded Nickel Nano-Composite Strain Gage

Timothy Michael Johnson
Brigham Young University - Provo

Strain Monitoring of Carbon Fiber Composite with Embedded Nickel Nanocomposite Strain Gage

Timothy Johnson

A thesis submitted to the faculty of
Brigham Young University
in partial fulfillment of the requirements for the degree of

Master of Science

David T. Fullwood, Chair
Anton Bowden
Mark Colton

Department of Mechanical Engineering

Brigham Young University

June 2011

ABSTRACT

Strain Monitoring of Carbon Fiber Composite with
Embedded Nickel Nanocomposite
Strain Gage

Timothy Johnson
Department of Mechanical Engineering
Master of Science

Carbon fiber reinforced plastic (CFRP) composites have extensive value in the aerospace, defense, sporting goods, and high performance automobile industries. These composites have huge benefits including high strength to weight ratios and the ability to tailor their properties. A significant issue with carbon fiber composites is the potential for catastrophic fatigue failure. To better understand this fatigue, there is first a huge push to measure strain accurately and in-situ to monitor carbon fiber composites. In this paper, piezoresistive nickel nanostrand (NiNs) nanocomposites were embedded in between layers of carbon fiber composite for real time, in situ strain monitoring. Several different embedding methods have been investigated. These include the direct embedding of a patch of dry NiNs and the embedding of NiNs-polymer matrix nanocomposite patches which are insulated from the surrounding carbon fiber. Also, two different polymer matrix materials were used in the nanocomposite to compare the piezoresistive signal. These nanocomposites are shown to display repeatable piezoresistivity, thus becoming a strain sensor capable of accurately measuring strain real time and in-situ. This patch has compatible mechanical properties to existing advanced composites and shows good resolution to small strain. This method of strain sensing in carbon fiber composites is more easily implemented and used than other strain measurement methods including fiber Bragg grating and acoustic emissions. To show that these embedded strain gages can be used in a variety of carbon fiber components, two different applications were also pursued.

Keywords: carbon fibers, nano composites, smart materials, strain sensing, in situ

ACKNOWLEDGMENTS

I would like to thank the many people who have helped and supported me in this endeavor. First, to my sweet wife for her countless hours spent testing, tutoring, editing, and studying with me. Second, I would like to thank my committee Dr. Colton, Dr. Bowden and especially to Dr. Fullwood, my committee chair. Next, special thanks go to Nate and George Hansen and Conductive Composites Company for their support in materials, lab time and technical expertise. Also acknowledgements in BYU Mechanical Engineering would not be complete without thanking Kevin Cole for all of his help and support on the hardware and software of this research.

TABLE OF CONTENTS

LIST OF TABLES

LIST OF FIGURES

1 CARBON FIBER COMPOSITES

Carbon fiber reinforced polymer composites have become widely used in many industries as a structural building material due to their mechanical, thermal, and electrical properties. While the ability to monitor fatigue in composite structures is vital to the growing industry, the current methods are less than adequate. Before fatigue can be better understood in carbon fiber composites, the methods of measuring strain must be better suited for carbon fiber composites. This research presents new methods for real time, in situ strain monitoring by the use of a piezoresistive embedded nanocomposite patch. This section gives a background of carbon fiber composites, an overview of their material properties, an introduction to the existing methods of sensing strain in carbon fiber composites and their limitations.

1.1 Background

Compared to many engineering materials and methods, the reinforcement of polymers with continuous carbon fibers is a very new principle. Carbon fibers have only been around since their relatively recent discovery by Bacon in 1958 [1]. It took several years to investigate, and several decades to come up with good methods of manufacturing. Today carbon fiber composites are a huge industry and because the cost of manufacturing is continually being reduced, the industry is expanding to new applications [2]. The industry is growing so quickly in fact that over the past 4 years the demand for carbon fiber composites has increased more than 225 % [3].

Carbon fibers are valuable because of their unique properties such as high Young's modulus, thermal and electrical conductivity, and tensile strength [4, 5]. The use of carbon fiber reinforced polymers allows the designer to manipulate bulk material properties such as Poisson ratios, coefficients of thermal expansion, and elastic modulus while reducing weight compared to conventional materials. This is because the strength can be put in the directions where it is needed without extra strength in other directions [6, 7]. Composite structures also show excellent material properties in toughness and fatigue [8]. These properties make carbon fiber composites a valuable material. Figure 1-1 shows an SEM image of carbon fibers.

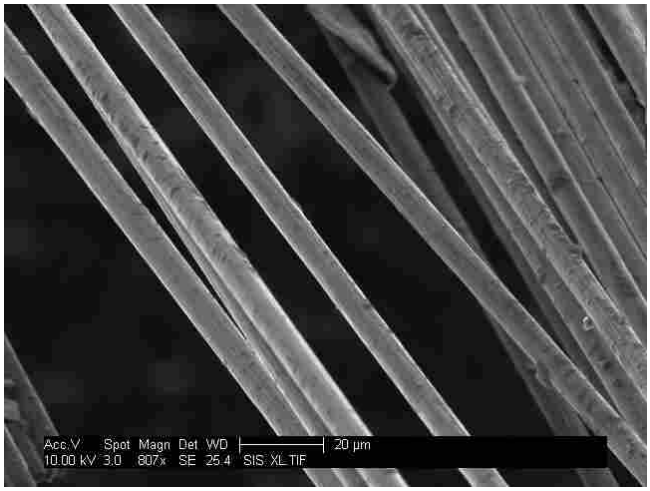

Figure 1-1: SEM Image of Carbon Fibers

Many industries such as the aerospace, defense, automotive, sporting goods, etc. are utilizing carbon fiber technology every day at an increasing pace [3]. Understanding failure mechanics and better predicting fatigue problems in composite structures by measuring strain accurately and in-situ will help to increase the applications and safety of carbon fiber composites.

1.2 Mechanical Failure Sensing in Carbon Fiber Composites

Carbon fiber reinforced polymers are a very valuable material; however, they do have some limitations. Unlike homogeneous materials such as metals where the properties of failure and fatigue are well understood, it is hard to predict failure in fiber reinforced materials. The main issue faced by composite users is that carbon fiber composites will have delamination, matrix cracking or other types of fatigue occurring inside the composite. This can be hard to monitor because it is not visible from the outside [4]. The ability to easily and unobtrusively measure the strain in situ becomes a key to the growing future of carbon fiber composites. For this reason a lot of research is being done to investigate methods of strain measurement in composite structures. A few valuable strain sensing methods in carbon fiber composites include traditional strain gauges, Raman wavenumber sensing, piezoresistive self-sensing, acoustic emissions sensing, and fiber Bragg grating. Although all five of these strain sensing techniques can give some detail about the fatigue of a composite structure, they have their drawbacks.

1.2.1 Traditional Strain Gages

Traditional strain gauges are mostly made out of thin strips of metal foil which changes resistance as the foil is strained. The change in resistance can be calibrated to accurately show strain in carbon fiber composites. These strain gauges are very effective in laboratory settings, but are less effective for in situ strain monitoring because they are simply glued to the surface. This means they are susceptible to damage, they can fall off (especially at high strain rates), and the wiring can be complex and messy for many sensors. These are seen as a relatively low cost type of strain measurement with gages being purchased for only a few dollars each.

1.2.2 Raman Wavenumber Sensing

Raman sensing shines a laser onto the surface of a material and detects the wavelengths and intensities that are reflected. Certain materials, when they undergo a strain, the reflected wavelengths and intensities will change. This powerful technique can accurately measure not only strain, but also stress concentrations and micro-failure in the carbon fibers themselves. However, some materials do not exhibit a change in wavelengths and intensities when strained. This complex method is not the easiest to set up or use. It is infeasible for real-time in situ strain measurements [9], but has an important place in the understanding of carbon fibers.

1.2.3 Piezoresistive Self Sensing

Another main way that scientists are measuring strain in carbon fiber composites is the use of the small piezoresistivity of the fibers themselves. When a carbon fiber is strained, the small resistance of the fiber will undergo a slight change. This has been extensively investigated and proven as an inherent strain sensing method [4, 5, 10]. Besides measuring strain, other failure mechanisms have been accurately measured by the use of the piezoresistive self-sensing property of the carbon fibers; these include delamination, fiber fracture, and damage propagation [7]. The issue with these types of measurements is the amount of change in resistance is so small in the carbon fibers that it is difficult to measure and reproduce results.

1.2.4 Acoustic Emissions Sensing

Many researchers want to verify the results from other methods of strain sensing by an independent measurement method. In the work of Gao, he was unsatisfied with the ability of the piezoresistivity to measure micro-cracks in the polymer. In response, he combined the resistance measurement with acoustic emission to gain deeper insight into the composite failure mechanics

[11]. Acoustic emissions sensing is the use of very sensitive acoustic measurement to “hear” the failure propagation of the composite. When a composite structure is pulled in tension the failure of fibers can be easily heard by the human ear, but acoustic emission keeps a count of every noise that the carbon fiber is putting off. The researchers that are employing this method find it very valuable to further the understanding of what is happening in the fatigue of the composite [5, 11-13]. On the other hand this method is extremely difficult in situ due to ambient noise in real world applications.

1.2.5 Fiber Bragg Grating

Fiber Bragg grating uses embedded fiber optics which, when strained, change the transmission of light which passes through the fiber. A grating is created inside the fiber in order to manipulate the laser light as it passes through it. Figure 1-2 shows a diagram of this grating before and after being strained.

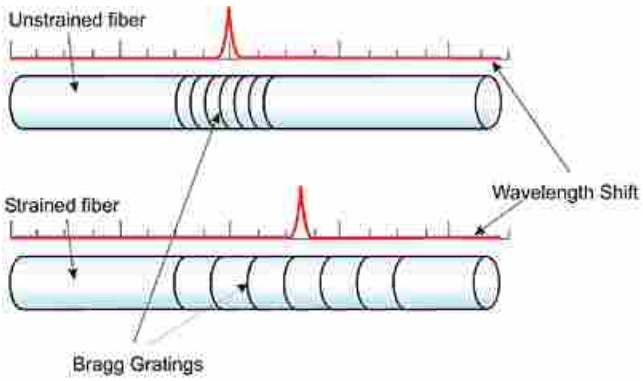

Figure 1-2: Diagram Showing Fiber Bragg Grating Method [14]

By calibrating the wavelength shift to the strain, accurate and repeatable measurements can be taken real time in situ. The optical measurements can be taken from a great distance away and the fibers can monitor not only strain, but temperature, pressure and chemical agents [14].

However, the implementation of this type of strain measurement method can be expensive and time consuming. The fragile fiber optic lines have to be embedded into the structure during manufacture or fixed to the structure afterward. The method is also susceptible to failure due to damage of the optical fibers themselves. Despite these issues the method is being successfully used by researchers [14, 15] and in some industry applications [14].

Although all five of these strain sensing techniques can give some detail about the fatigue of a composite structure, they have their limitations. Table 1-1 shows a summary of the strengths and weaknesses of many of the strain measurement techniques available.

Table 1-1: Comparison of Existing Strain Monitoring Methods

Existing Methods	In situ?	Easy?	Cost?	Sturdy?	Alter Prop?
Foil strain gauges	yes	med	low	med	med
Piezoresisitivity of Carbon Fibers	no	no	med	yes	no
Raman Wave-Number	no	no	high	yes	no
Acoustic Emissions	no	med	med	med	no
Fiber Bragg Sensors	hard	no	high	no	med
Embedded Carbon Black	yes	med	low	yes	yes
Embedded CNT	yes	med	med	yes	yes

The piezoresistive method is the cheapest and least complex to use real time in situ, but the changes in resistance are very small, as mentioned above. Therefore, more research is still needed to find better strain sensing methods for in situ strain measurements of carbon fiber composites. The ideal method would be easy to employ, non-destructive, accurate for small strain, and would introduce minimal amounts of stress concentration. Some nanocomposites have mechanical and electrical properties that seem promising for piezoresistive measuring of strain in carbon fiber composites.

2 NANOCOMPOSITES

The term nanocomposite refers to any material made from the dispersion of nanoparticles into a polymer matrix. In order to understand how nanocomposites can be used to sense strain in carbon fiber composites, an understanding of nanoparticles and their properties is needed. The background on a few different types of nanoparticles will be discussed, along with how these nanoparticles can be used to reinforce mechanical properties, enhance electrical conductivity, and create piezoresistive strain sensors.

2.1 Types of Nanoparticles

Carbon black, carbon nanotubes/nanofibers, and nickel nanostrands (NiNs) are all used in nanocomposites. In this section these types of nanoparticles will be discussed, their history briefly overviewed, and their properties and uses elaborated.

2.1.1 Carbon Black

Carbon black is a very popular micro and even nano particle that has been used for nearly one hundred years in many industries. Although it was discovered in 1865 by an ink maker, J. K. Wright, the technology to cost effectively produce carbon black would not be sufficient until the early 1900's. Carbon black is made by the burning of natural gas which contains too much

hydrogen sulfide. Although the process uses large amounts of natural gas, this gas represents only a very small percent of the total natural gas used today.

The small carbon particles can be used as a filler to help with the stiffness and durability of rubber. By 1915 it was being used in most automobile tires. It can also be used as a pigment in paints and some inks. Today there is still a huge demand for this nano-particle; trillions of tons of carbon black are produced every year for these and other purposes.

In many ways carbon black has been a stepping stone to the uses of nanoparticles today. Many researchers are finding that other particles such as CNT and NiNs can replace carbon black and achieve much better results. The main reason for this is that these other particles are much stronger and much more electrically conductive than the carbon black particles. This is due to their structure, the chemical makeup, and extremely high aspect ratio of the CNTs and NiNs. Gojny and his research group compared the fracture mechanics of an epoxy reinforced with carbon black vs. CNTs. The benefit with CNT is that similar strength can be achieved with a very small amount of CNTs compared to carbon black [16].

2.1.2 Carbon Nanotubes/Nanofibers

Carbon nanotubes were discovered by Iijima in 1991 [17] and have since created a lot of excitement in material science and engineering. There are several types of carbon nanoparticles that are being used and are available on the market. These include single walled carbon nanotubes (SWCNT), multiple walled carbon nanotubes (MWCNT), and carbon nanofibers (CNF). The SWCNT and MWCNT are very popular in many fields of scientific research and have unlimited industrial applications [9, 16, 18]. The carbon nanofibers, on the other hand (CNFs), are much less discussed due to slightly different structure and properties. They generally have much more microstructure defects than the other carbon nanotubes [18].

Each unique property of CNTs has created quite a flurry of research. Due to the pure carbon lattice structure, CNTs are the strongest material ever made to date [18, 19]. They also are extremely good conductors of electrical current and heat [20]. Nanoparticles can have aspect ratios of 1000 m^2/gram [16] or more, which is nearly a quarter acre of area per gram. For the most part these tubes are not elaborately branched in structure but are relatively singular and straight, as shown in Figure 2-1.

Figure 2-1: SEM Image of CNTs [21]

CNTs are being distributed into other materials to enhance their bulk mechanical and electrical properties [22, 23]. This leads to many novel applications for CNTs.

2.1.3 Nickel Nanofibers

The next type of nanoparticles, which is much less known, but even more pertinent than CNTs, is nickel nanostrands (NiNs). These fibers are created by the Conductive Composites Company in Heber, Utah. The Conductive Composites Company is a family business in the Heber, Utah area [24]. The owner and operator of the company is George Hansen. His wife and

children also help him run the business and perform their own in-house research. The nanostrands are created by a proprietary chemical vapor deposition (CVD) method at their Heber Utah fabrication facility. They have been commercially selling their NiNs since 1995. They graciously support many universities in the area including Brigham Young University, Utah State University, and the University of Utah. They have donated nickel nanofibers to many research groups in the past few years [25-28].

The nickel nanofibers are also very high aspect ratio nanostrands [24]. They have a distinctive bifurcated, or two branched, micro-structure as seen in Figure 2-2 [28].

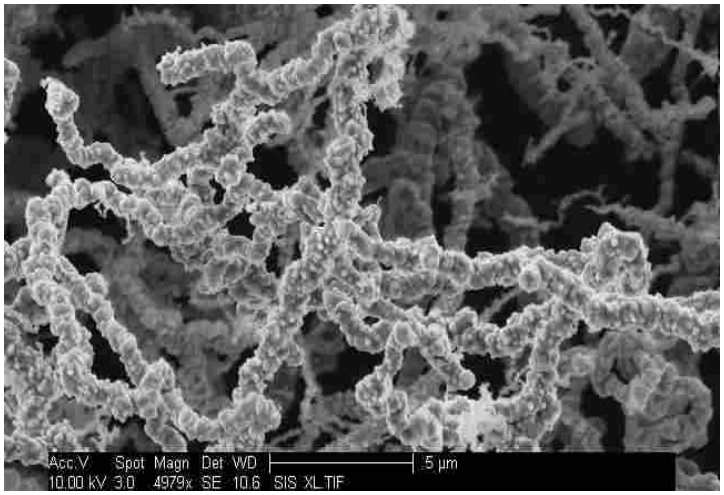

Figure 2-2: SEM Image of NiNs

Besides the good branched structure, these NiNs have a high modulus and high conductivity as well as being easily aligned under relatively low magnetic field compared to trying to align CNTs [25]. This structure makes them different from the long single shafted CNT structure. The NiNs are also much more brittle in nature than CNTs [25]. This means that mixing methods must be very different and these dispersion issues will be discussed later. With the unique microstructure of the NiNs there are also many unique applications of these particles.

2.2 Electrical Conductivity

Historically, to make a polymer conductive carbon black was often used. However, due to the huge electrical conductivity of CNTs and NiNs, researchers are optimizing mixtures and alignment of these nanoparticles in a matrix material in order to achieve a good electrical conductivity through the entire structure. This can occur at very low percentages of nanoparticles [29] compared to the high percentages of carbon black required. These electrical properties are enabling CNTs and NiNs to replace carbon black in some industrial applications [16].

A common application of both CNTs and NiNs is the creation of electrical shielding materials. When they are mixed into a polymer, the resulting conductive plastic material can be used to encase sensitive electronics from static discharge [24]. CNTs and NiNs can also be mixed into a coating, such as paint or polyurethane, and applied to the outside of a structure to electrically shield [30] it against lightning strike, on a plane for example [24, 29]. This coating can be simply sprayed on with a standard paint sprayer [31].

2.3 Reinforcement of Mechanical Properties

CNTs can be mixed into many materials to increase mechanical properties, such as strength and toughness, especially in fracture mechanics [16]. For example, in one research group lead by Wagner the Young's modulus was increased up to 28% higher for a rubbery polymer matrix at weight percentages as low as 1% of CNTs. In a different mixture of a "glassy" epoxy Young's modulus was unchanged, but a huge 50% increase in impact toughness was shown [32]. These groups have been putting huge efforts into understanding the wetting characteristics, mechanisms for micro-adhesion, stress transfer to and from CNTs and matrix material, as well as developing ways to measure the interfacial strength [23]. One research group found that by introducing CNTs into a polymer matrix the resultant nanocomposite would much

more efficiently dampen mechanical vibrations [15]. This is an important mechanical property due to the many high vibration situations that engineered components encounter.

CNTs are so strong that even tiny volume fractions in a nanocomposite will greatly stiffen the mechanical properties [16]. This can be desirable in some cases, but as an embedded sensor it is necessary to leave the mechanical properties of the composite unaltered. For this purpose the use of NiNs, shown in Figure 2-3, is more advantageous.

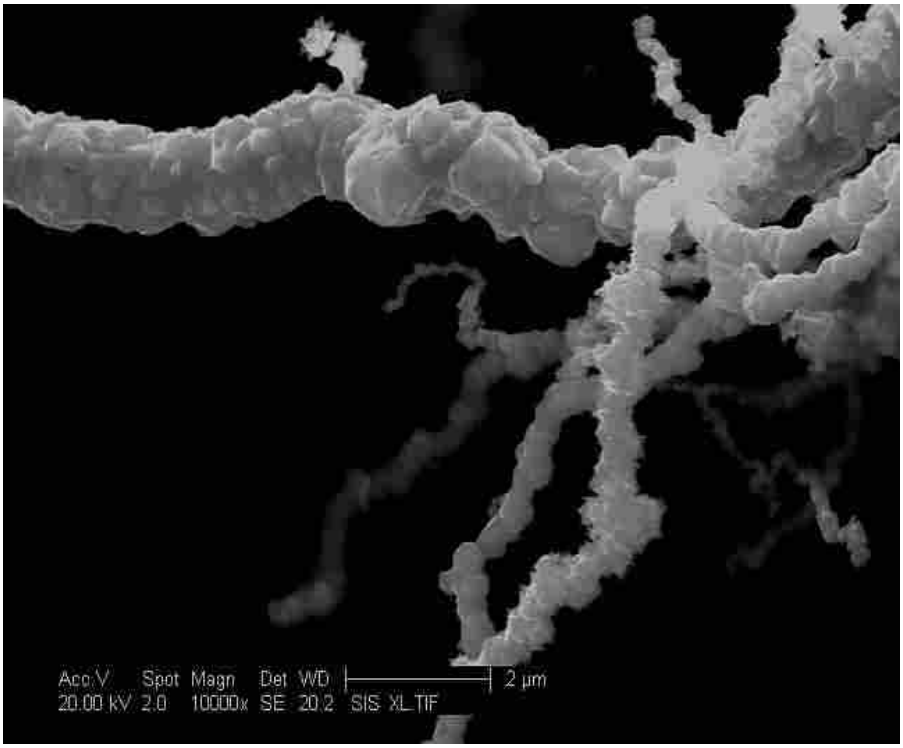

Figure 2-3: SEM Image of NiNs

They have a much more fragile microstructure which reduces the amount of stress concentration they introduce when used as an embedded sensor.

Because nanoparticles are already being used as fillers to manipulate mechanical and electrical properties in many applications, it seems a simple transition to using them for other applications.

2.4 Piezoresistive Strain Sensing

For the purpose of this research the most applicable use of nanocomposites is the ability to sense strain. On even a single CNT the resistance of the tube will change large amounts as it undergoes deformation as applied with an atomic force microscope [9]. But what is more interesting is the phenomenon which occurs when a nanocomposite is formed with these nanoparticles in a polymer matrix; the overall nanocomposite then shows huge piezoresistivity [20, 28, 33, 34]. A lot of research is being done on how these nanocomposites can measure not only strain, but micro-damage, and stress transfer preceding failure [12, 35].

One specific research is that of Oliver Johnson also at BYU [27, 28, 36]. He has not only fabricated effective NiNs/Silicone nanocomposite strain gages, but has also investigated in depth the percolation and quantum tunneling mechanisms which explain this piezoresistivity, as will be discussed later. Figure 2-4 shows the high strain response from the NiNs/Silicone gages he was making [36].

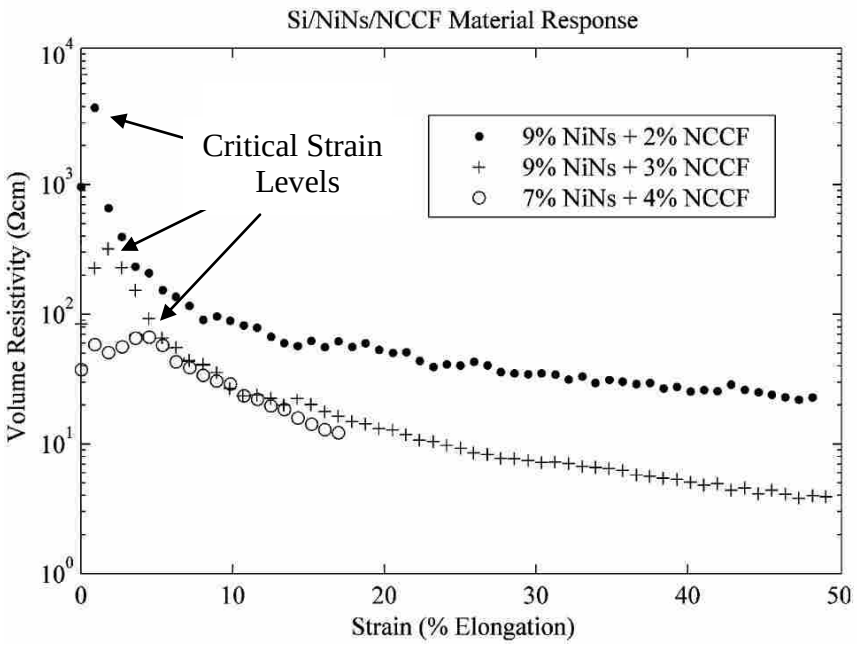

Figure 2-4: Resistivity Response of Si/NiNs/NCCF Strain Gages (duplicated with permission [36])

Although Johnson achieved good piezoresistivity at high strain, low strain response was not investigated in his research. For each of the nanocomposite gages tested the resistivity first increases and then at some critical strain level the resistance drops. In his research Johnson was introducing the Nickel Coated Carbon Fibers (NCCF) in order to reduce or eliminate this knee in the response.

To understand the piezoresistive response of nanocomposite strain gages, some background on percolation theory and quantum tunneling is useful. Therefore, a brief summary is provided here; for more detail see the following citations [9, 20, 22, 27, 28, 33, 36, 37].

Percolation theory is generally depicted as a series of points and connecting lines as in Figure 2-5. The points are referred to as "sites" and the connecting lines are referred to as "bonds". For many sites in a given region there is some probability that two adjacent sites are or are not bonded. In a given region there is a critical probability which will result in a bonded network which spans the region; this value is referred to as the percolation threshold. [36]

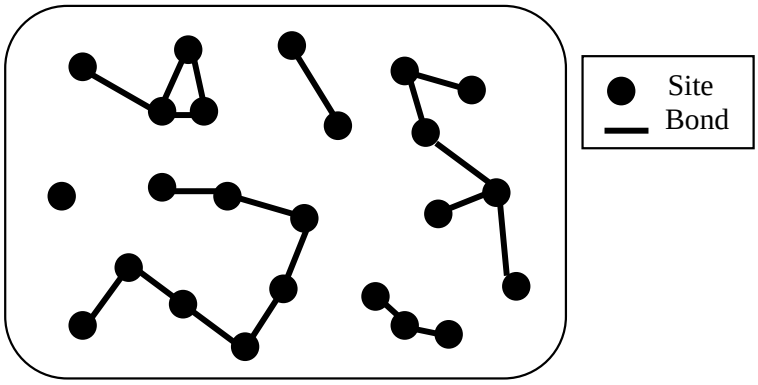

Figure 2-5: Diagram Illustrating Percolation

Electrically this threshold, on a large scale, is found when the nanocomposite transitions to conductive from non-conductive. Generally this will appear as the curve in Figure 2-6, where the resistivity dramatically decreases when the bond probability reaches the percolation

threshold. The simplest way to manipulate the bond probability is to increase or decrease the volume percentage of nanoparticles. For NiNs it takes less than one volume percent to reach the percolation threshold.

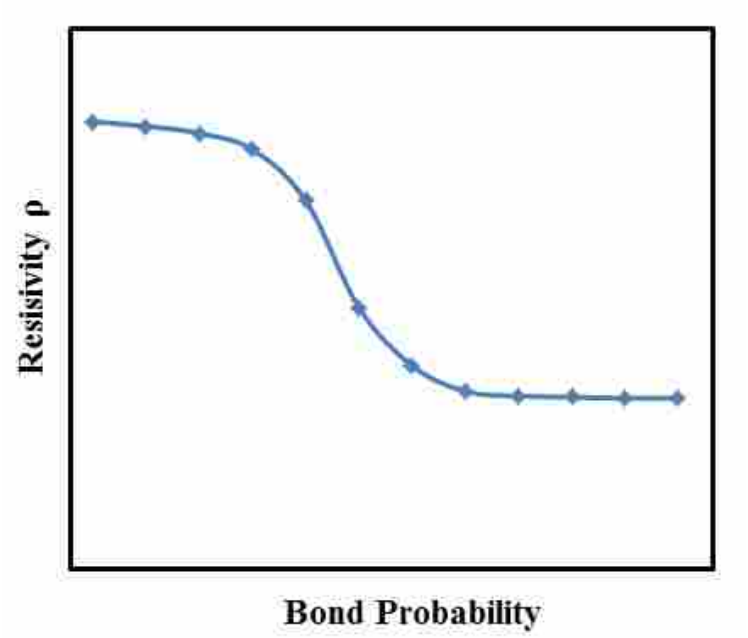

Figure 2-6: General Percolation Curve

Next, to understand the flow of electrons in the nanocomposite a brief look at quantum tunneling will be presented. In quantum tunneling when an electron encounters a physical barrier in its flow path, such as the polymer matrix slightly separating two conductive NiNs, there is some probability that the electron will actually pass through that barrier. Figure 2-7 shows a regular bell curve representing the probability of an electron being on either side of the barrier.

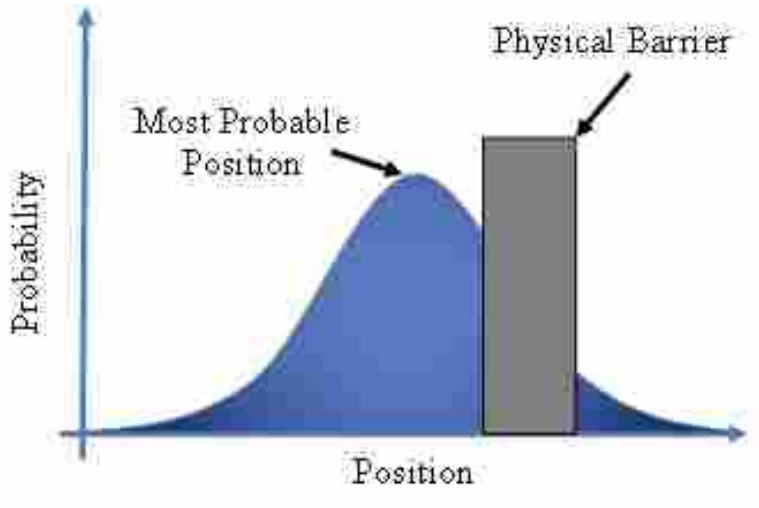

Figure 2-7: Quantum Tunneling Probability

This quantum tunneling effect is occurring in many nanocomposites. In the case of piezoresistive NiNs nanocomposite strain sensors, there are many conductive NiNs (i.e. sites) separated by the polymer. In order for current to pass through the physical barrier by quantum tunneling (i.e. the sites are bonded) the barrier thickness must be below about 5 nm. The regions of space where two adjacent nano-particles are close enough that there is the potential for quantum tunneling to occur are referred to as nano-junctions. The flow of electrons is dependent on whether these nano-junctions are or are not bonded; this can easily be affected by placing the nanocomposite into a state of stress. The resulting strain acts in such a way as to change the physical barrier width in these nano-junctions, closing the bond in some nano-junctions, and opening, or unbonding, it in others. In a given strain state a large number of nano-junctions will open with very few closing while another strain state will result in a larger number of nano-junctions being closed while very few open. Therefore, in this type of strain sensor, it is not uncommon to encounter strain gages which either increase or decrease resistance, depending on loading conditions. In the research of Oliver Johnson in Figure 2-4, the resistivity first increases, meaning that more of the nano-junctions are unbonding during this period of strain; then at the

critical strain value where the resistance drops there is a dramatic decrease in gap size of the nano-junctions [36]. This increase in bonding has been attributed to the Poisson effect forcing the NiNs closer together.

Percolation helps quantify when enough nano-particles are dispersed into the polymer that many nano-junctions are formed. With enough nano-junctions, the overall nanocomposite displays piezoresistivity when the nano-junctions are altered by the strain state.

Previous research has focused on the piezoresistivity of the nanocomposites themselves and has little to do with the use as embedded sensors in carbon fiber composites. Both CNTs and NiNs in a nanocomposite have been shown as a valuable way to measure strain [28, 33], however introducing CNTs/polymer nanocomposite into carbon fiber composites would create an extremely stiff strain gage patch resulting in high stress concentration. In the case of NiNs/Polymer nanocomposites the mechanical stiffness of the nanocomposite does not exceed that of the carbon fiber composite itself. Therefore, the NiNs were selected as a better fit for use as a nanoparticle filler in a piezoresistive nanocomposite strain gage for embedding in carbon fiber composites.

3 RESEARCH OBJECTIVES

With the increasing demand of carbon fiber composites in many industries, the need for a better strain monitoring method is crucial as was discussed previously. This strain monitoring would provide the composite industry the ability to better predict and avoid catastrophic failure, which failures have stunted this market in the past. The demand for carbon fiber could then become more stable and expand into new applications resulting in lowered cost of carbon fiber and the potential to utilize these promising materials in a wider range of products.

The objective of this research is to create NiNs piezoresistive nanocomposites and embed them in between layers of carbon fiber composite for real time, in situ strain monitoring.

To this end, several nanocomposites and different embedding methods have been investigated. These include the direct embedding of a patch of dry NiNs and the embedding of NiNs-polymer matrix nanocomposite patches which are insulated from the surrounding carbon fiber. Also, two different polymer matrix materials were used to compare the piezoresistive signal.

In order for these strain gages to be validated, they need to: 1) exhibit good piezoresistive signal quality at low strain; 2) show potential for calibration; 3) give repeatable resistance measurements through many cycles and between different gages; and 4) last for many strain cycles. It was also of interest to measure the resistance signal as the carbon fiber composite was

failed. To show that these embedded strain gages can be used in a variety of carbon fiber components, two different applications were also pursued.

It is not the purpose of this research to fully define the limitations and applications of this technology, but simply to prove the validity of it and show that it is worth pursuing in more detail.

4 EXPERIMENTATION

The experimentation needed to investigate the application of NiNs nanocomposites in strain sensing in carbon fiber composites will be discussed in this section. This includes the materials used, the sample preparation, and the mechanical and electrical testing methods.

4.1 Materials

To construct these sensors, the main materials include the NiNs, two part epoxy, silicone rubber, and both carbon and glass prepreg. The NiNs are the conductive filler used to create the piezoresistive nanocomposite. The two part epoxy and silicone are used as the matrix material in these nanocomposites. The fiberglass prepreg is used in some samples to electrically insulate the strain sensor from the carbon fiber prepreg.

4.1.1 Nickel Nanostrands

The NiNs that are used in these experiments are created by the Conductive Composites Company in Heber, Utah. Figure 4-1 shows an SEM image of these NiNs, taken by the author. These particles have very unique properties and structure, such as high conductivity, huge aspect ratios as well as complex microstructure.

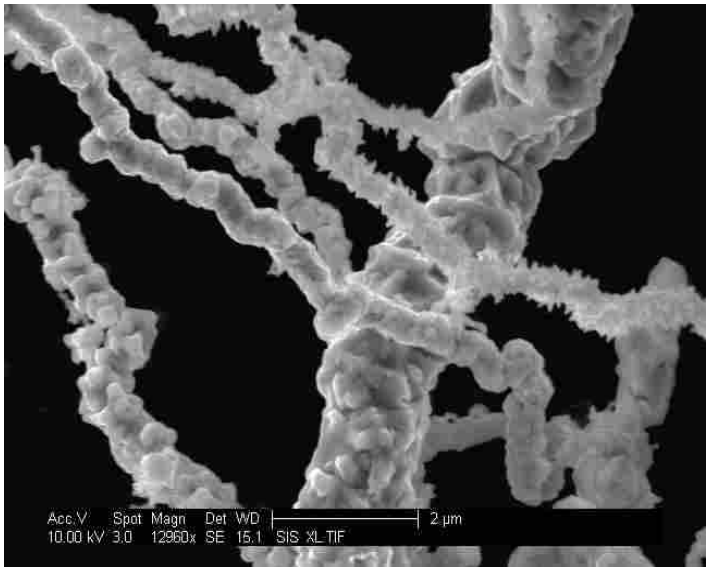

Figure 4-1: SEM Image of NiNs

To prepare the nanostrands, a simple screening method is used with a 60 mesh screen (250 micron spacing) in order to ensure a more uniform conglomeration size. The nanostrands are then weighed on a gram scale with 0.001 gram accuracy.

4.1.2 Epoxy and Silicone Rubber Matrix Materials

The epoxy was a room temperature cure two-part epoxy from West Systems® known as 105 Resin with a 209 Hardener for its longer pot life. The silicone rubber was a Dow Corning's® two part silicone elastomer, Sylgard 184.

4.1.3 Carbon Fiber and Fiberglass Prepreg

The carbon fiber prepreg used in these tests was donated to Brigham Young University by Hexcel Co. The unidirectional fibers are a M50JB6K type with a 3501-6 epoxy matrix. The prepreg is cut to shape for the samples and laid up by hand. The published cure cycle for this prepreg material was used in an autoclave. The fiberglass prepreg used in this research was a

SP381 7781 0ST type in a plain fabric weave. For applications of the nanocomposite patches, a plain fabric weave carbon fiber prepreg was also used. It was an AGP 370 type again with a 3501-6 epoxy matrix.

4.2 Sample Preparation

Several different types of carbon fiber composite test samples were prepared for this research. These include directly embedding a piezoresistive patch in between layers of carbon fiber prepreg and insulating the patch with fiberglass before embedding it in carbon fiber. Both embedded sensor samples and control samples with no sensor were made. Also, samples were designed for testing in tension and in bending.

4.2.1 Directly Embedded Patch Samples

The first type of embedded sensor is made by the placement of a patch of dry NiNs between layers of unidirectional carbon fiber prepreg. Following screening and weighing, the nanostrands are placed in a 19 mm by 12 mm patch between two of the layers of carbon fiber prepreg. Therefore, the amount of NiNs in these sensors is measured in a weight per patch area. This method depends upon on the prepreg matrix epoxy flowing around the NiNs to produce a good nanocomposite. Wire leads are not connected to the embedded patch because of the higher conductivity of the unidirectional carbon fibers compared to the matrix epoxy. These carbon fibers act as wires allowing the signal to be measured down the length of the sample. The carbon fiber test samples were then cured and tabs were applied for gripping in the tensile tester. These grips are necessary not only for holding the sample securely, but also for insulating the conductive carbon fiber from the metallic grips of the tensile tester.

The applications of this embedded sensor are limited to unidirectional carbon fiber because for other layup patterns the signal short circuits through the carbon fiber. To further extend the application of this type of embedded sensor to layup patterns other than unidirectional carbon fibers, the nanocomposite patches can also be insulated from the carbon fiber by fiberglass prepreg and wires inserted for the signal to be measured, as will be discussed. Insulating the nanocomposite patch also opens the possibility for greater nominal resistance and, thus, larger piezoresistive magnitude.

4.2.2 Insulated Patch Samples

In the case of insulating the patch, the sample preparation is very different. There is a layer of fiberglass prepreg on both the top and bottom of the nanocomposite patch. In order to contain the nanocomposite, there is also a layer of fiberglass prepreg with a rectangle cut out of the center of it as in Figure 4-2. The nanocomposites can be easily spread into this compartment, wires inserted into it, and the final layer of fiberglass placed on top. This entire subassembly can be placed in between layers of carbon fiber prepreg and cured. The insulated samples were slightly wider than the directly embedded samples in order to better fit the glass prepreg subassembly, while leaving the nanocomposite patch at the same width of 19 mm.

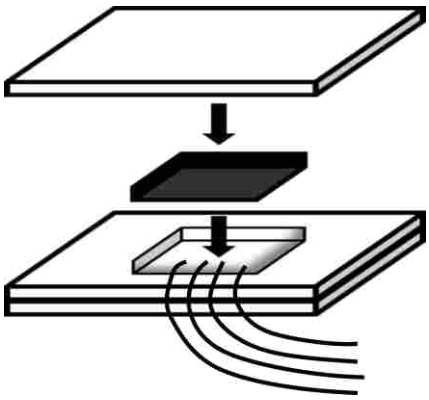

Figure 4-2: Illustration of Nanocomposite Patch Insulated in Fiberglass Prepreg

The first of the nanocomposites that were used in this arrangement was 9% by volume NiNs mixed into the two part epoxy described above. The nanocomposite was spread into the insulating compartment instead of being directly embedded as the dry NiNs were.

Silicone rubber was also used as an insulated nanocomposite patch matrix material at a volume fraction of 15%. The dispersion of the NiNs in both insulated samples is performed in a THINKY® planetary mixer for 10-20 seconds. The limited mixing time preserves the bifurcated microstructure of the NiNs. For both nanocomposite types the volume fractions were selected based upon previous work [36].

In general the dispersion of nano-particles in a polymer matrix is much more difficult than is alluded to here. More understanding of the methods and tools for small particle dispersion is required to prove that the THINKY® mixer with a short mixing time is ideal. A discussion of many techniques along with their benefits and drawbacks is given in more detail in Appendix A. It is sufficient to say at this point that the THINKY® planetary mixer is the best fit for the NiNs.

4.2.3 Bending and Tension Sample Preparation

While the NiNs nanocomposite patches were prepared the same way for both tension and bending samples, there were differences in the carbon fiber placement and size during the sample preparation. For tension type samples the NiNs patch was placed in the middle of all the layers, four above and four below. On the other hand, this type of sample would not work for bending due to that location being the neutral axis. Therefore, the NiNs patch was placed on just one layer of prepreg, and then fourteen additional prepreg layers were placed on top of that. Therefore, these samples were thicker which provided better bending stiffness.

All of the NiNs nanocomposite patch samples for bending were 25 mm wide and 300 mm long. However, in tension there were different sample sizes. The insulated NiNs nanocomposite

patch samples were again 25 mm wide, but without having to encase the fiberglass insulating patch the directly embedded samples were only 19 mm wide.

4.3 Testing Methods

Following sample preparation, the objective was to: 1) investigate whether the carbon fibers in a regular carbon fiber composite can be used to electrically connect the embedded NiNs sensor to the measurement device; 2) produce resistance curves for various patch configurations in order to design the optimal piezoresistive gauge; and 3) validate the utility of directly embedded sensors as well as the insulated sensors via resistance tests on samples as they undergo known strain.

4.3.1 Resistance of Carbon Fibers to be used as Wires to NiNs Patch

For the directly embedded sample, the effectiveness of using the carbon fibers for the wires is tested by measuring the resistance at a location other than directly over the embedded NiNs patch. Resistance measurements were taken using the four probe method. This method has four collinear probe tips, passing a known amount of current through the sample via the two outer probes, and measuring the voltage drop over the two inner probes. To calculate resistance the voltage drop is then divided by the amount of current. By ensuring that current does not have to flow over the two center probes the contact resistance of these probes is entirely eliminated from the measurement [38].

4.3.2 Percolation Resistance Measurements

For the directly embedded dry NiNs, it is first important to understand how many grams of NiNs are needed. There should be enough NiNs to form a large number of nano-junctions

which facilitate the piezoresistivity of the gages. To quantify this, a series of samples were tested which had varying amounts of NiNs directly embedded into them. The shape of the resistance curve will help to ensure that the sample is well percolated, and thus has a sufficient number of nano-junctions.

4.3.3 Tensile Tests

To prove the validity of measuring strain via embedded NiNs patches, the carbon fiber samples were pulled in tension in an Instron® tensile tester as shown in Figure 4-3.

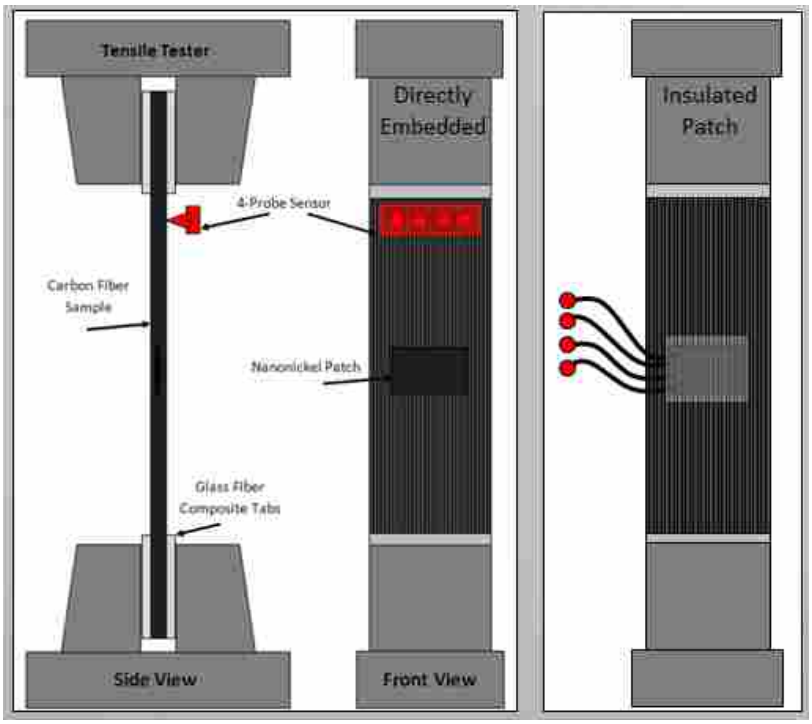

Figure 4-3: Side and Front Views of Sample in Tensile Tester with Embedded Sensor

This tester is instrumented with a dynamic load cell and accurate displacement controls. The displacement, force, and resistance data (by four probe method) were recorded and compiled for each test. Cyclic load cycles were performed at varying frequencies. Strain levels of 0.25% and 0.5% were used to measure piezoresistivity with the embedded sensor.

Possibly the biggest difficulty of performing tensile tests with carbon fiber composites is slippage in the tensile tester grips. The hardened steel grips are generally textured to dig into tensile samples. This can be detrimental to carbon fiber composite testing because when the grips dig into the sample the fibers near the edge are broken. This causes the sample to fail inside the grips. Therefore, the samples are generally fitted with thicker tabs at the ends as stated in the ASME standard [39].

For the purpose of this research the complexity is exaggerated by the need to electrically insulate the test samples from the metallic grips. Different tab materials and different methods of attaching those tabs were used in this research with varying degrees of success. First, tabs cut from thin fiberglass sheets were attached with superglue or epoxy. These worked until the test exceeded certain load values. Plastic sheets attached with a higher strength epoxy were also tried, but once again only worked to a certain load.

Figure 4-4 shows the force/displacement graph when the samples slip in the grips. The sharp drop in load during the first cycle is when the slipping occurs. As the sample slips, the length of sample between the grips increases. Therefore, as the tensile tester returns to its original position the sample goes into compression. Due to the thin sample size, the sample buckles under the compressive load.

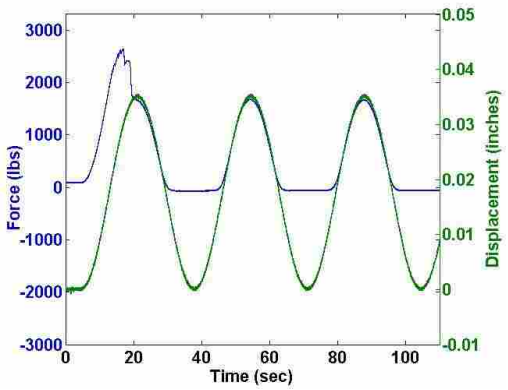

Figure 4-4: Force and Displacement Graph Showing Sample Slippage

To resolve this issue, a more complex layup method was employed in which the carbon fiber prepreg strips were fitted with fiberglass prepreg tabs on the ends and both materials were cured together. This cured adhesive bond proved much stronger than the previous methods and no slipping or buckling occurred.

4.3.4 Bending

In order to investigate the resistance response of these embedded NiNs nanocomposite strain gages in bending, a three point bend arrangement was implemented as illustrated in Figure 4-5. The samples were placed on two lower supports and a wedge was brought down in the middle causing the sample to bend. The resulting stress is such that the upper fibers are forced into compression while the lower fibers, where the embedded patch is located, are forced into tension.

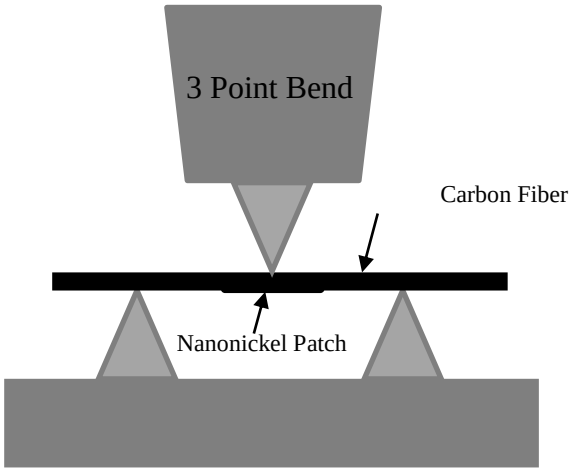

Figure 4-5: Diagram Showing 3-Point Bend Arrangement

The ASME D790 standard was consulted for different parameters including spacing of lower supports, radii of the supports and wedge, and the initial strain rates. The strain of the bottom-most fiber layer is given by Equation 4-1.

$$\varepsilon_f = \frac{6Dd}{L^2} \tag{4-1}$$

Where ε_f is the strain, D is the vertical displacement of the wedge, d is the depth or thickness of the test sample, and L is the distance between the lower supports.

The three-point bend method was used which is a well established ASTM method for which the equipment was available, but 4-point would possibly give a more consistent result due to the better stress profile in the region of the gauge.

4.3.5 Electrical Measurement Methods

For the methods of strain measurement that require electrical resistance measurements, there are several methods for taking these readings. Some of the measurement techniques include a standard two terminal method, four terminal, and the simultaneous measurement of strain by other means. It is important when selecting a method of measurement to take into account the amount of change in resistance that is expected, the resolution of measurement that is desired, and the contact resistance of the sample. For example, some nanocomposites can have fairly negligible contact resistance due to the high conductivity of the surface of the sample, but on the other hand a carbon fiber prepreg sample will have huge surface resistance compared to the resistance of the sample itself.

The two-terminal-method is the simplest measurement to set up and take. A direct measurement with an ohm meter would fall into this category. The ohm meter is sending a known current through the sample and measuring the voltage drop through the same two probes.

This means that the contact resistance is still in the measurement, which may or may not be an issue [20]. When the changes in resistance may be small a voltage divider circuit can be used to amplify the signal received by the ohm meter. The principle of voltage dividing is a well-established measurement technique [28, 40].

In the case that surface resistance is an issue the best technique to eliminate the contact resistance is the widely used four terminal method [4]. The four terminal method of resistance measurement has been around since Lord Kelvin in 1861 [38]. It uses four separate terminals or probes in a linear pattern. The outer two probes apply a known current though the sample. The inner two probes measure the drop in voltage across the nanocomposite patch. Due to the high impedance of the voltage probes, essentially no current flows through the two center probes; therefore, the contact resistance is eliminated entirely from the measurement [38, 41, 42]. Finally, using Ohms law the resistance across this portion of the sample will be calculated from the current applied and the voltage drop measured. This method is extensively used especially by researchers using carbon reinforced polymer composites [4, 10]. This is due to the high resistance matrix which is coating the fibers. With these proven methods the measurement of resistance change can be accurately taken.

In order to take these four probe resistance measurements, a data acquisition (DAQ) board was used. It was a National Instruments Ni cDAQ-9172 carriage with a Ni 9219 module. This is a multi-function module capable of resistance measurements. A four probe setting was used, so that the DAQ would output resistance directly into LabView. The DAQ in this setting passes 500 μA through the outer two probes, and measures the drop in voltage over the inner two probes. The DAQ performs the calculation of ohms law to read resistance to the screen:

$$R = \frac{V}{I} \tag{4-2}$$

The DAQ has an input impedence of 1 MΩ to ensure that neglegable current will flow through the voltage probes. In the resistance measurement setting the DAQ has a gain error of ±0.1% of the reading and an offset error of ±120 ppm of the full 10 kΩ range. Due to the reletively low speed of testing, the DAQ was set to record data at a sample rate of 100 Hz which was sufficient. The DAQ has two settings for resistance measurements: high resolution and high speed. For the high resolution, the level of noise is minimized by signal averaging over a certain number of data points. This is discussed in further detail in Section 5.4.

A LabView interface recorded the resistance from the DAQ as well as the analog signals of displacement and force from the tensile tester. This data was all compiled into separate files for each test for further analysis.

The placement of the four probes is critical to measure the resistance of the embedded patch. For the directly embedded NiNs samples, to use the carbon fibers to carry the electrical signal to the probes are placed in a colinear pattern perpendicular to the unidirectional carbon fibers. Figure 4-6 shows these four probes which were made with simple needle tips held in place by acrylic strips. These probes do not cause any significant damage to the composite structure, and therefore, seem to be a practical method. For most of the testing, these probes were placed directly above the embedded patch, or very close to it.

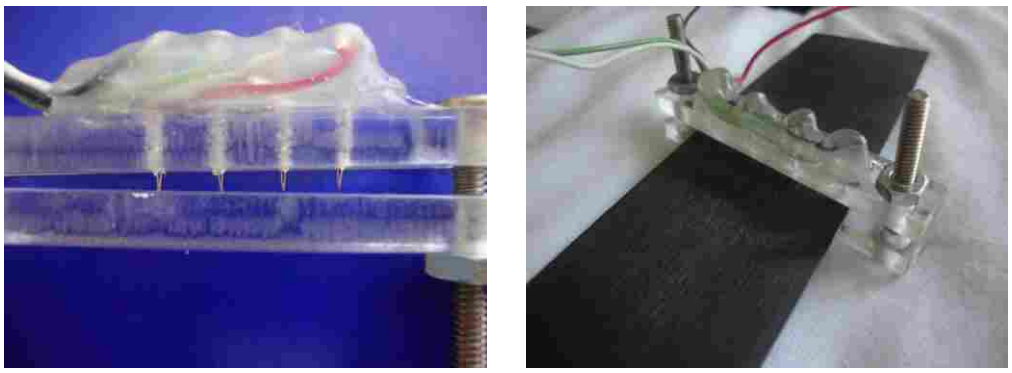

Figure 4-6: Images showing Four-Probe Resistance Measurement Method

For the insulated NiNs nanocomposite samples, four wire leads were brought out of the embedded NiNs patch as shown in Figure 4-2. These leads were connected directly to the DAQ for the resistance measurements. Because the four probe resistance measurement is being used and the impedance of the DAQ is so high, the resistance of these leads is not a factor in the signal measurement.

5 RESULTS AND DISCUSSION

Through the given testing methods, data was collected for control samples, directly embedded NiNs sensors and the insulated NiNs/Silicone and NiNs/Epoxy nanocomposite sensor types. The viability of the different types of nanocomposite strain gages was investigated along with the strain measurement quality, signal repeatability, calibration, nanocomposite fatigue and signal during carbon fiber sample failure. NiNs/Epoxy nanocomposite embedded sensors were applied in both a carbon fiber prosthetic foot as well as a drive shaft to demonstrate the viability of the method in actual composite components.

5.1 Control Sample

With no embedded NiNs strain gage, the change in resistance of a carbon fiber composite while being strained is negligible. A representative graph of the resistance measured from unidirectional carbon fiber composite tension control samples is shown in Figure 5-1. According to research performed by Wang and Todoroki, the changes in resistance in carbon fibers would be on the order of micro-ohms [4, 10], which is consistent with our results.

After these confirming results for tension samples, control samples were then tested in bending. During bending it is understood that the bottom half of the sample goes into tension and the top into compression. The four probe measurements were taken on the bottom most fibers of the sample.

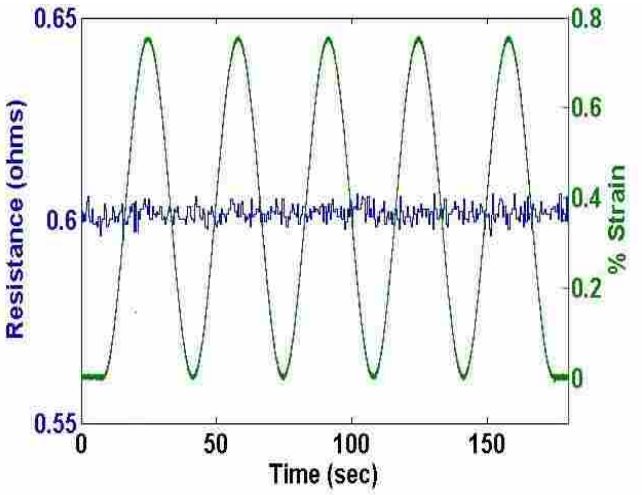

Figure 5-1: Tensile Sample without NiNs

Remembering that the current is more likely to flow down the fibers than through the thickness, it is still valuable to see that there are no significant changes in resistance of the sample during bending. Figure 5-2 shows results for a representative bending control sample at 0.5% strain. The instrument accuracy cannot measure any change in resistance. Several different control samples showed similar flat lines when tested at different strain amounts and different strain rates.

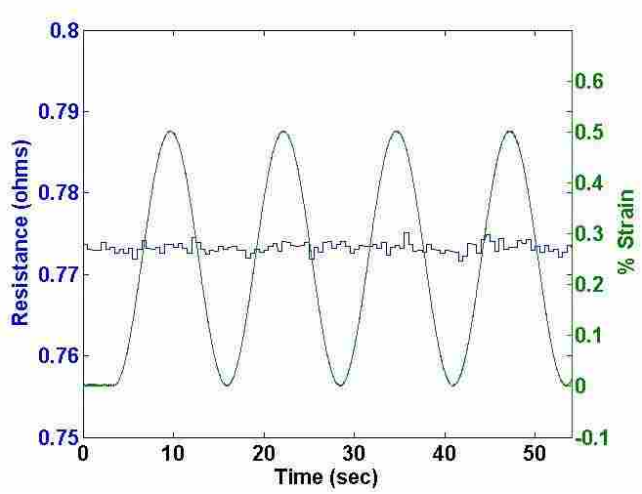

Figure 5-2: Bending Control Sample without NiNs Patch and 0.5% Strain

5.2 Direct Embedding of Nickel Nanostrand Patch

Following these control sample results, directly embedded NiNs patch samples were tested to see if significant resistance change could be measured showing that this type of gage is possible. Before this could be done, some results showing the effect of using the carbon fibers as wires and the amounts of NiNs needed in a directly embedded patch are given.

The graph in Figure 5-3 shows that there is a simple relationship for the resistance between the probes as they are moved away from a conductive patch, down the length of the unidirectional fibers. The unstrained resistance of this patch is only 0.3 ohms as is shown at the y-axis intersection of this graph. Figure 5-3 shows that with the overall composite resistance of about 0.7 to 0.8 ohms, the additional resistance of the carbon fibers would make the piezoresistive signal indiscernible by at most 70 cm. To measure a significant signal, it may only be reasonable to measure the piezoresistive signal at a distance of about 30-40 cm away from the patch.

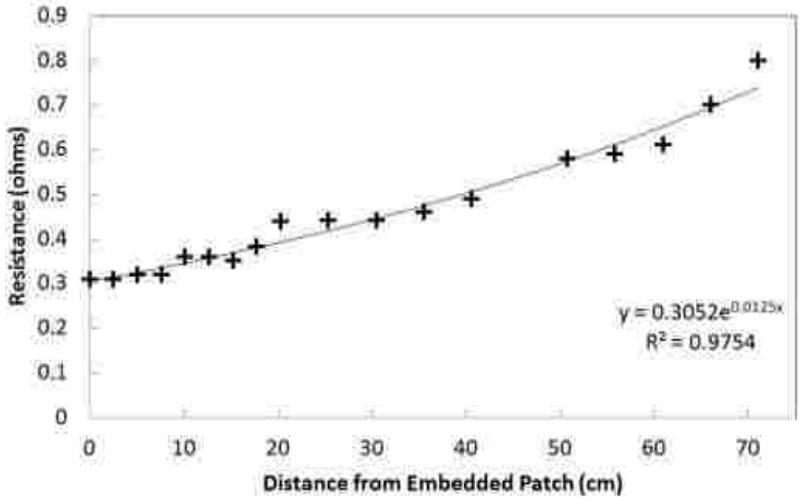

Figure 5-3: Resistance vs. Distance down the Carbon Fibers to the Embedded Nanocomposite Patch

On the other hand, the measured resistance is a function of spacing of the four probes on the surface of the sample. If a wider spacing was used, perhaps greater distance could be achieved, but this would also require a larger embedded patch size. For the testing of the directly embedded NiNs gages in this research the signal was measured very near the patch. Therefore, no wires were placed in the unidirectional test samples. This eliminates stress concentration due to the wires and simplifies the layup process.

The theory of using the unidirectional carbon fibers as the wires requires that the signal is more likely to pass down the fibers through the nanocomposite patch and back to the measurement probes than directly across the matrix material. When a more complex layup pattern is required, the current tends to short out. This is verified by the results in Figure 5-4. This was the straining of a sample made with a $[0/90/0]_S$ layup pattern directly embedding the NiNs between the [0] center layers. The first indication that the current is shorting out through the carbon fiber is the level of resistance measured. Besides having a resistance value more than an order of magnitude lower than usual, it is clear that the piezoresistivity of the embedded NiNs cannot be measured.

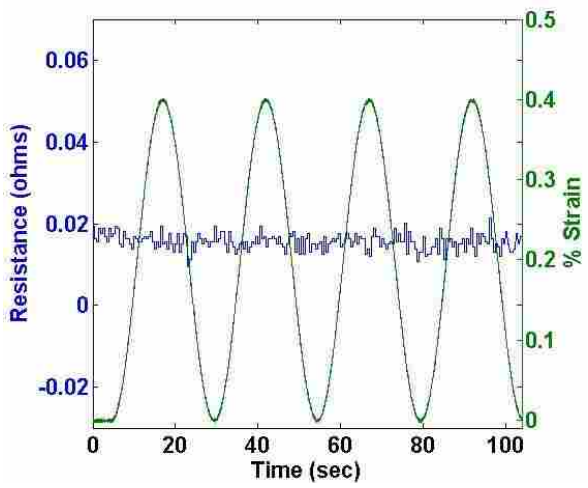

Figure 5-4: $[0, 90, 0]_S$ Layup with Directly Embedded NiNs Showing Shorting of Electrical Signal

The amount of NiNs needed for a directly embedded strain gage with good piezoresistivity is going to be where the sample is well percolated. This allows for many nano-junctions to be present in the sample that can be bonded or unbounded under strain. Therefore, for the directly embedded NiNs patch, a resistance curve for different amounts of NiNs is given in Figure 5-5. The curve shows that compared to the resistance of only the carbon fiber, shown at the y-axis intercept, the resistance of the samples even with only 0.01 g of NiNs is lower. At these amounts of NiNs the samples are percolated which means there should be many nano-junctions to provide the piezoresistive effect.

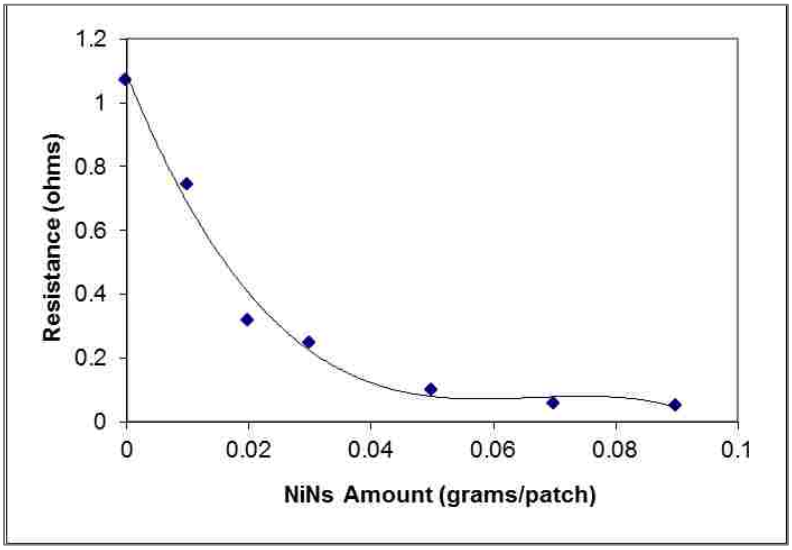

Figure 5-5: Resistance of Samples as a Function of Weight per Area of NiNs in the Embedded Patches

After straining each of the samples represented in Figure 5-5 in tension, results from 0.01g and 0.03g are shown in Figure 5-6. It can be seen that at these levels of NiNs the signal is indiscernible.

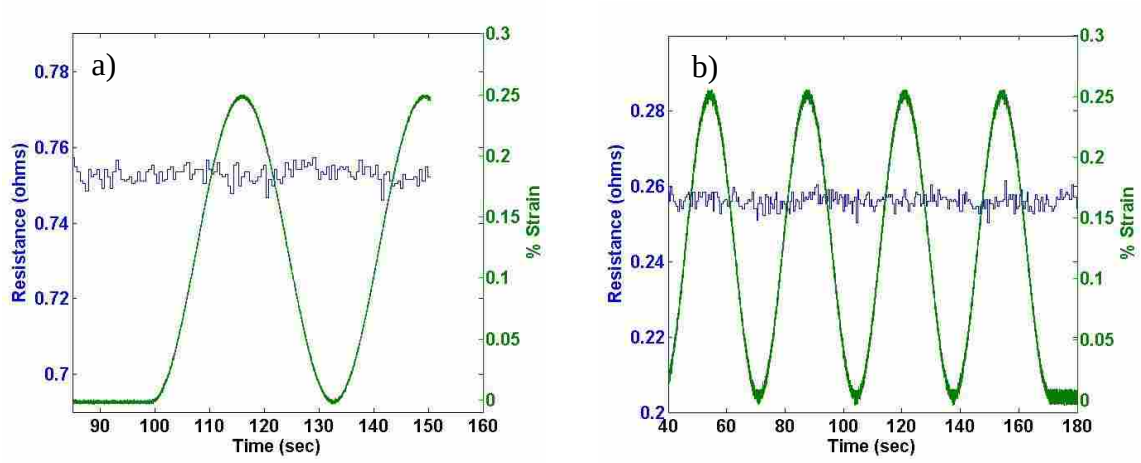

Figure 5-6: Resistance Measurement a) 0.01g NiNs Patch and b) 0.03g NiNs Patch

However, the 0.02g of NiNs per patch was found to be effective for piezoresistive use and its resistance measurements are shown in Figure 5-7. There is a significant amount of resistance change with each strain cycle, indicating that this NiNs patch can be used as a strain gauge and embedded directly into unidirectional carbon fibers. For samples with less NiNs it could be that there are insufficient nano-junctions to display any measurable change in resistance. On the other hand for the samples with higher amounts of NiNs there are already so many connected junctions that adding strain does not appreciably change the resistance.

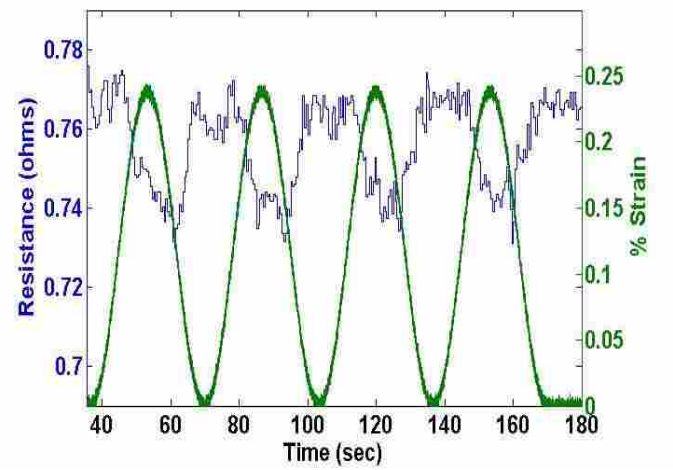

Figure 5-7: Directly Embedded NiNs (0.02g per patch)

Similar results were also produced on the tension surface of the bending tests. These samples were flexed at different strain rates and to different strain values. Figure 5-8(a) shows a representative plot of resistance change and strain over several cycles. To show how well the resistance signal reflects the strain in the sample, Figure 5-8(b) displays the inverted resistance signal with the strain.

It is valuable to notice that this signal, although it is small, is easily discerned by the data acquisition system and this simple embedded NiNs patch shows great potential to be used as an embedded strain gage for carbon fiber composites.

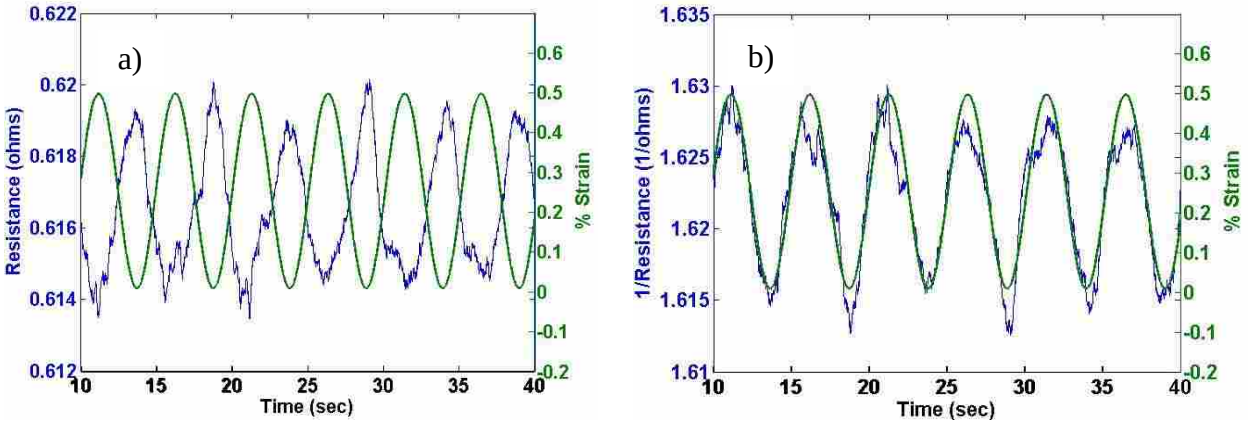

Figure 5-8: Directly Embedded NiNs Bending Sample a) showing the Resistance Change and b) showing the Resistance Signal Following Strain

For the directly embedded NiNs to properly form a nanocomposite the nanostrands must be saturated by the excess epoxy on the carbon fiber prepreg. During the regular cure cycle of the carbon fiber prepreg, before ramping to 177 ºC, the temperature first holds at 121 ºC where the epoxy can become less viscous and can flow around the nanostrands. Because excess epoxy is generally pulled from carbon fiber composite as it is cured, it was assumed that there would be enough epoxy to fully saturate the NiNs. Several SEM images were collected of a cross section

of carbon fiber composite with the embedded NiNs. Due to the non-conductive nature of the epoxy it tends to electrically charge from the microscope beam. This charging gives a shiny look to the epoxy helping to visualize where it has or has not saturated the NiNs. In Figure 5-9 the upper section of the image shows well saturated NiNs, but the lower region is free of epoxy showing dry NiNs.

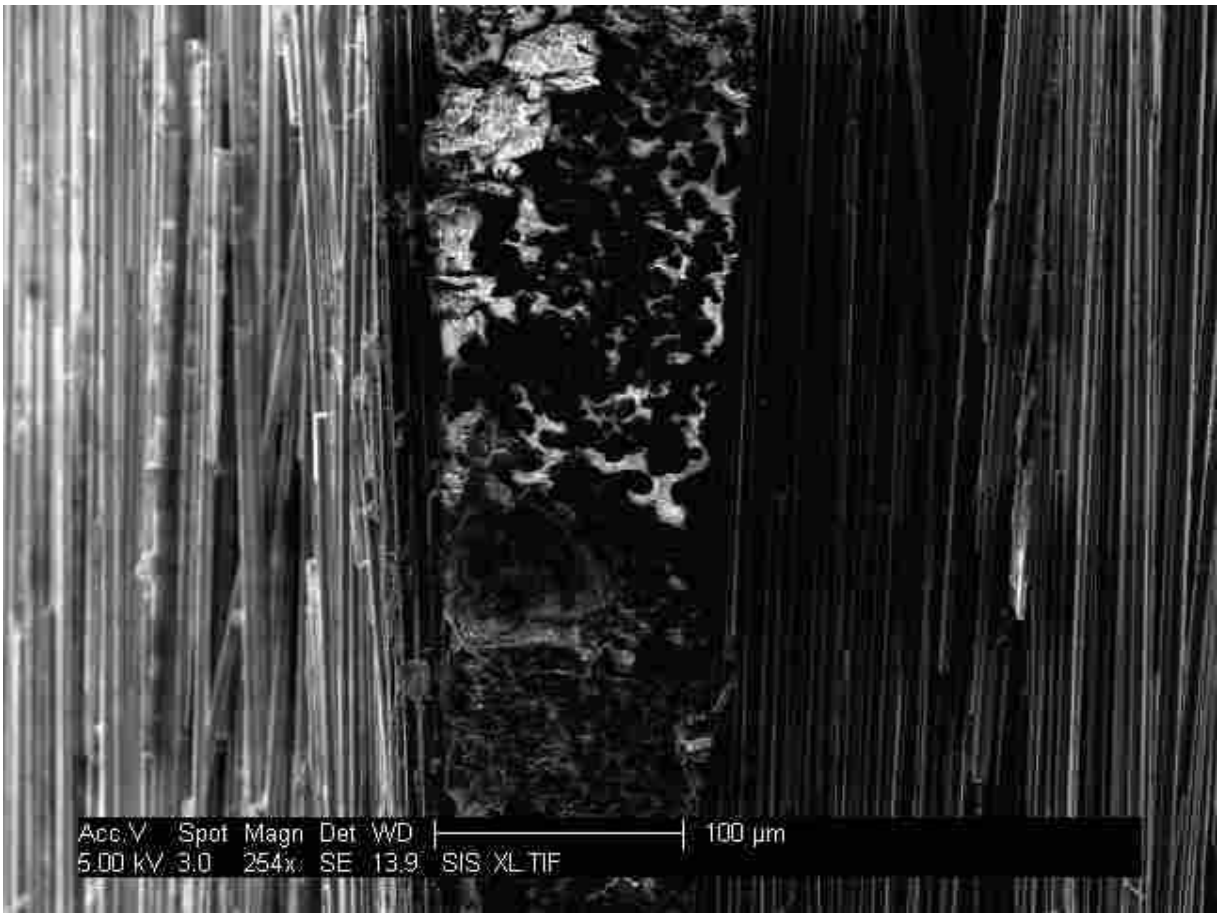

Figure 5-9: SEM Image of Cross Section of Directly Embedded NiNs

The presence of dry NiNs is detrimental to the nanocomposite piezoresistivity. This is because without saturating the nanostrands, it is unclear how nano-junctions will be formed or altered during strain. While the actual percentage of NiNs being saturated is unknown, there are obviously enough nano-junctions being formed to show the piezoresistivity measured, as in

Figure 5-8. More work should be done in the future to facilitate better NiNs saturation. This may also point toward the mixing of the NiNs in an epoxy prior to directly embedding in between the carbon fiber prepreg.

5.3 Embedding of Insulated Nickel Nanostrand Nanocomposite Patch

In addition to the directly embedded samples, the insulated patch samples also show significant piezoresistivity. This extends the application of these embedded sensors to non-unidirectional carbon fiber composites. Results are given first for the NiNs/Silicone nanocomposite embedded patch followed by the NiNs/Epoxy patch samples.

5.3.1 Insulated NiNs/Silicone Nanocomposite Patch

The resistance signal from an embedded NiNs/Silicone nanocomposite patch undergoing cyclic loading to 0.25% strain in tension is shown in Figure 5-10. With this low level of strain a change in resistance of 0.01 ohms, from the upper and lower peaks of one strain cycle, is still seen. The rise in nominal resistance also seen in the plot will be discussed later in this section.

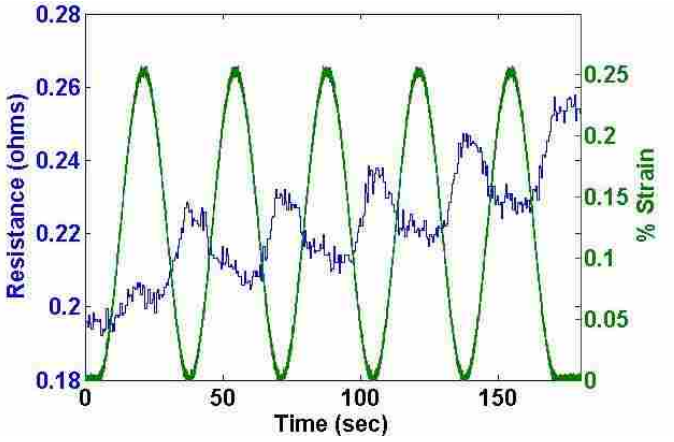

Figure 5-10: NiNs Silicone Nanocomposite Insulated from Carbon Fibers

In bending the NiNs/Silicone nanocomposite type of sample shows a more significant piezoresistivity, as shown in Figure 5-11, but calls attention to several interesting phenomenon which should be addressed for future designs.

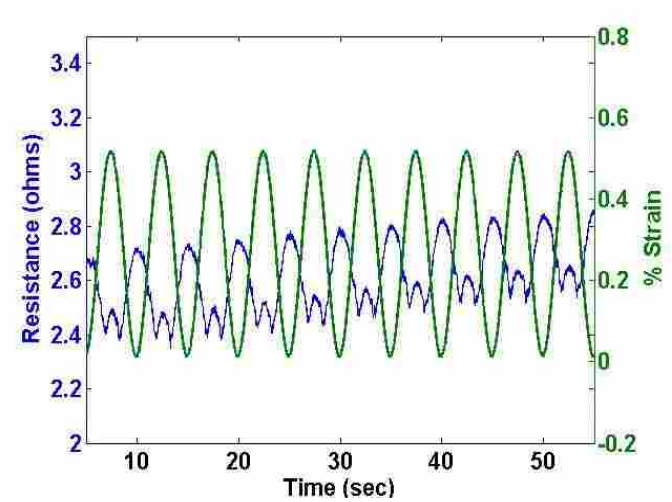

Figure 5-11: NiNs/Silicone Nanocomposite Signal Showing Double Cycle and Rise in Resistance

In the space of one strain cycle there are two significant changes in resistance. This phenomenon is similar to that shown by Oliver Johnson when the resistance curves change direction at a certain level of strain. On the other hand, it is clear that the signal is changing opposite in direction to that seen by Johnson by first decreasing followed by the increasing at higher strain [36]. It is hypothesized that this double cycle is due to the dominant loading state felt by the nanocomposite. During the first part of the cycle the tension dominates as shown in the top half of Figure 5-12 and the resistance drops, but as the strain increases the compressive loads in the sample become more dominant because of the tension in the carbon in the lower part of the beam, and the lower modulus of the patch. This is represented in the bottom half of the figure and in this loading case the resistance rises. Similarly, residual stress in the sample from manufacturing may also be playing a large role in this phenomenon.

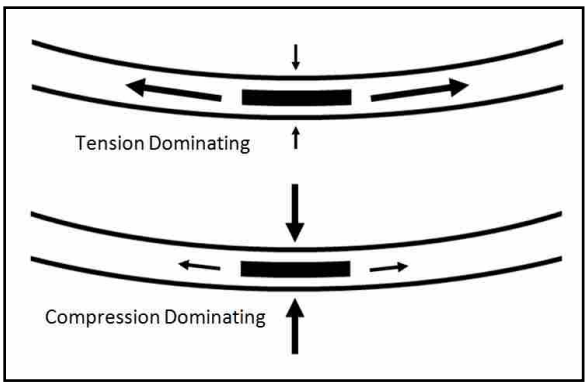

Figure 5-12: Dominant Loading Conditions in Embedded NiNs Strain Gage

The next interesting phenomenon shown by the NiNs/Silicone nanocomposite patches is the increase in nominal resistance and piezoresistive signal magnitude with the number of cycles. Figure 5-11 shows the climb in nominal resistance as the number of cycles increases and Figure 5-13 shows that sometimes the piezoresistive signal magnitude changes over many cycles. These signal features were hypothesized to be due to several possible effects, including electrical charging of the sample, reversible nanocomposite patch conditioning (e.g., viscoelastic effects), or irreversible damage to the embedded nanocomposite patch itself (e.g., creep of the matrix or fracture/displacement of the nano-strands). Each of these possibilities was investigated and will be explained below. It will be shown that NiNs fracture or displacement is the most likely cause.

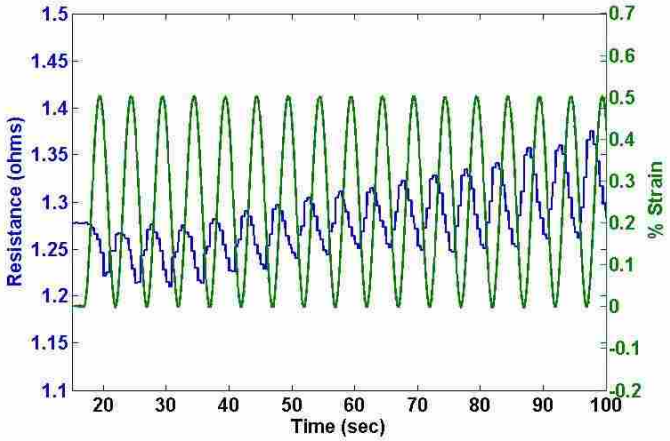

Figure 5-13: NiNs/Silicone Patch Showing a Rise in Resistance

By grounding the carbon fiber and the embedded nanocomposite patch between cyclic bending tests, charging of the sample was eliminated, but proved to make no difference in nominal resistance or piezoresistive magnitude. Therefore, electrical charging is not contributing to these signal abnormalities. To investigate the reversible nanocomposite patch conditioning, the sample was set aside for nearly two weeks and tested again. This time the sample resistance started slightly below the ending value from the previous tests and with the larger piezoresistive magnitude still present. This implies that a small amount of reversible material phenomenon is occurring.

On the other hand, most of the signal abnormalities are due to irreversible nanocomposite damage. To understand whether creep or fatigue is doing the damage it must be investigated whether time or number of strain cycles drives the resistance higher. A sample which was increasing resistance during 0.5% sinusoidal strain loading cycles was then held at 0.5% strain for a several minutes. Figure 5-14 shows the strain and resistance signals during that time.

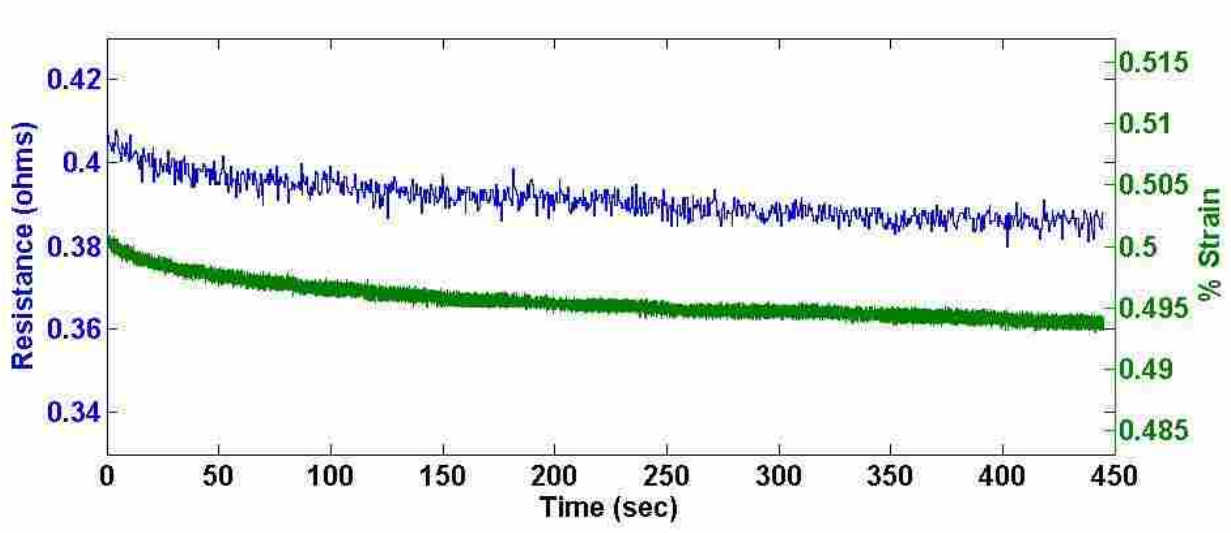

Figure 5-14: NiNs/Silicone sample Held at 0.5% Strain during an Interrupted Cycling Test

The strain and resistance drop slightly due to stress relaxation from the viscoelasticity of the epoxy in the carbon fiber composite, but the resistance is not continuing to rise as would be expected if creep were damaging the gage. Therefore, the rise in resistance is due to fatigue damage of the nanocomposite. This fatigue is due to either breakage or dislocation of the nanostrands. In the case of nanostrand dislocation the NiNs may be pulled out of position which dramatically changes the nano-junction width thus resulting in higher resistance and higher piezoresistive magnitude as has been seen.

5.3.2 Insulated NiNs/Epoxy Nanocomposite Patch

As opposed to the NiNs/Silicone type gages, the NiNs/Epoxy type is much more consistent. The tension signal shown in Figure 5-15 displays a measurable amount of piezoresistivity for this embedded gage. This sample was strained to 0.5% and the resistance changed a total of about 0.01 ohms.

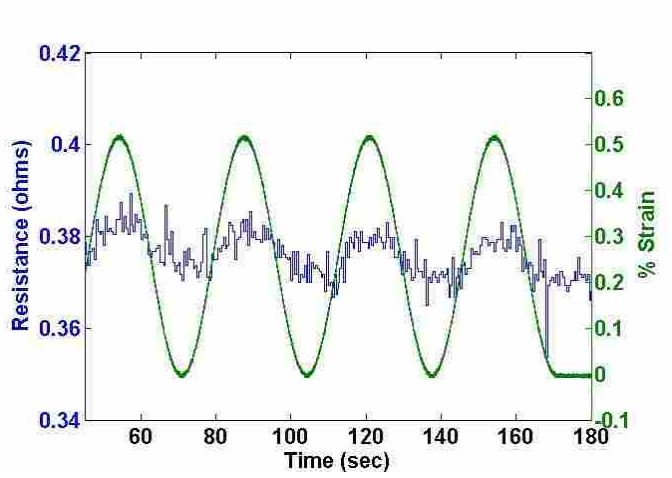

Figure 5-15: NiNs/Epoxy Nanocomposite Insulated from the Carbon Fibers during Tension Tests

Notice that for this type of gage the resistance increases with strain as opposed to decreasing with strain as in the other gage types. This appears to be more in line with the work of

Oliver Johnson where, at low strain levels, the resistance of the nanocomposite gages increased [36]. It could be that this type of nanocomposite is simply below the critical strain value (see Figure 2-4) where the resistance will decrease after that.

Once again, the bending samples displayed a larger piezoresistive magnitude as shown in Figure 5-16. While these samples also show some slight drift in nominal resistance, it is orders of magnitude less than the NiNs/Silicone type gage. In one case, over 3000 strain cycles were performed with no noticeable change in the nominal resistance. While this gage is much more consistent, some of the NiNs/Epoxy samples display lower piezoresistive magnitude than the NiNs/Silicone and therefore have lower resolution. Therefore, whether the application requires low strain levels with fewer cycles or higher cycle loading would determine which type of embedded nanocomposite strain gage would be better suited for the application.

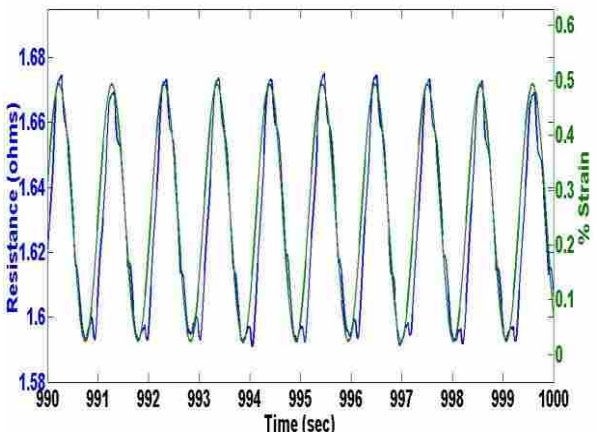

Figure 5-16: NiNs/Epoxy Nanocomposite Insulated from the Carbon Fibers during Bending Tests

While it was previously shown that there is some permanent damage in the nanocomposite structure of the NiNs/Silicone sample type, it seems that the NiNs/Epoxy type samples do not show this same damage. With the epoxy polymer being the most significant

difference in patch composition, it is clear that the epoxy is better preserving the piezoresistivity of the nanocomposite gage. This could be due to the higher modulus of elasticity of the epoxy compared to the silicone, thus protecting the microstructure of the NiNs from breaking. Also, the epoxy could simply be bonding to the nanostrands better than the silicone, therefore not letting the NiNs dislocate or slip out of place. In either case, the epoxy matrix material seems to better preserve the nano-junctions for long term strain monitoring in carbon fiber composites. A better understanding of how the epoxy is protecting the nanocomposite structure and function is something which could be researched in the future.

5.4 Strain Measurement Quality

With any type of strain gage, one of the biggest issues is resolution which means that the resistance must change measurably at low amounts of strain. As seen from Figure 5-17 there is an easily measured change in resistance at only two hundred fifty microstrain (0.25% strain) for this NiNs/Epoxy sample. Similar results were also recorded for NiNs/Silicone samples. This sort of resolution shows the potential of these sensors to measure strain in even relatively small strain applications.

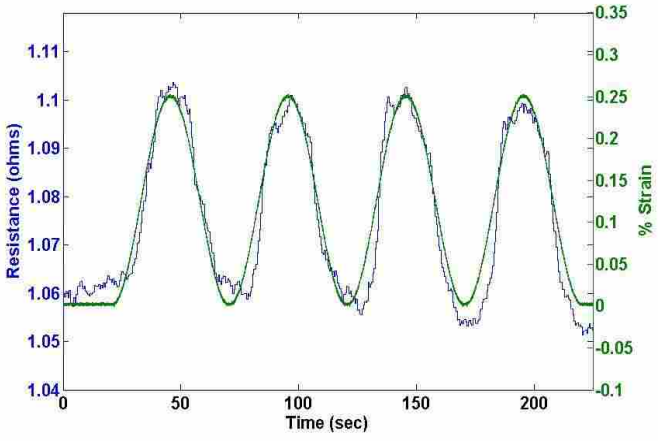

Figure 5-17: NiNs/Epoxy Nanocomposite Patch with .25% Strain

Another issue affecting the strain measurement quality is seen in Figure 5-18(a) where there appears to be a time lag in the resistance signal from the cyclic strain in the sample. A time lag would be undesirable for any strain gage. In contrast, Figure 5-18(b) does not seem to show any time lag. It is clear by the difference in signal that they were recorded in different ways. The first signal is very choppy and square while the other displays a high noise level. The data acquisition system (DAQ) used in the measurement of the resistance signal had two different settings for resistance measurements: high speed and high resolution.

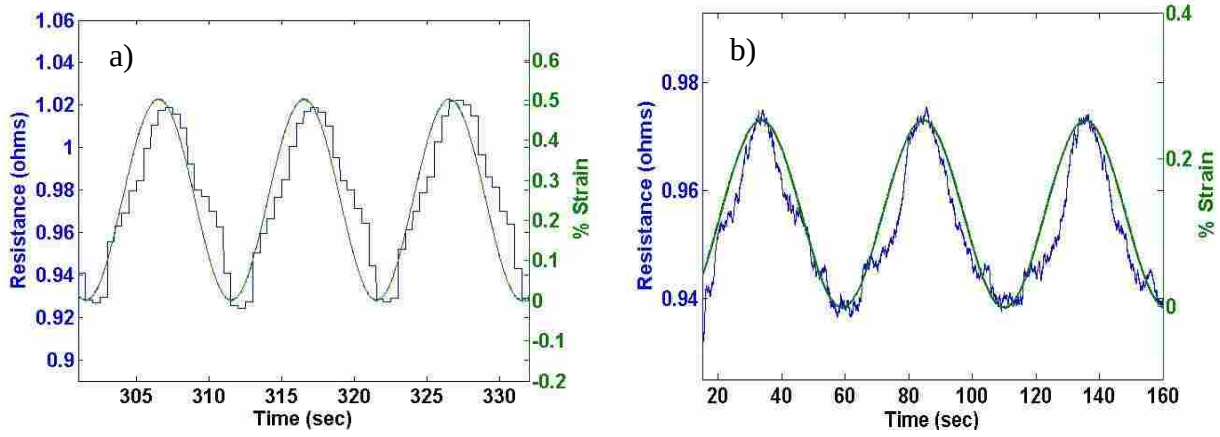

Figure 5-18: Different Resistance Measurement Recording Types: a) High Resolution and b) High Speed

To understand the source of this time lag it became important to determine how the DAQ was recording the choppy high resolution signal. By looking closely at the data compiled in the tests, it was seen that many data points were recorded at the exact same value for each of the choppy steps. To reduce noise in the signal, the DAQ performs a signal averaging on the data. When collecting data at a frequency of only 100 Hz, 50 data points were averaged and recorded as the same value, thus introducing a time delay of one half of a second as seen in Figure 5-19. Therefore, the signal time lag is due to the high resolution setting in the DAQ. While this time

lag is undesirable, the high resolution signal is much less noisy and was used in many of the lower speed tests.

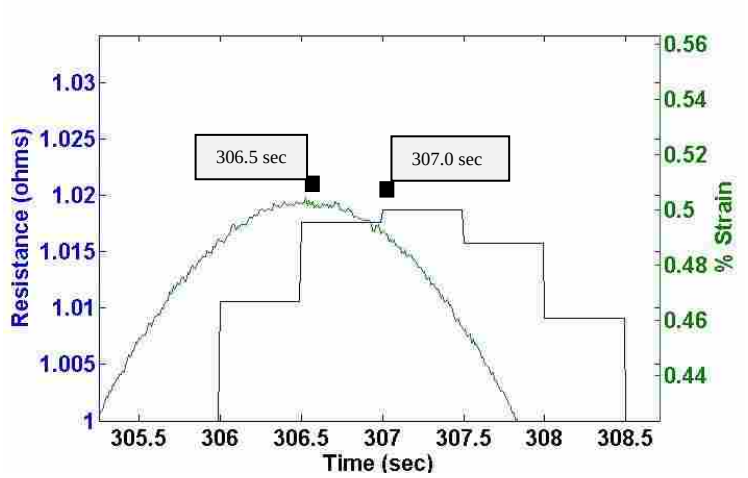

Figure 5-19: Half Second Time Lag shown from High Resolution Signal

While the resolution results are promising for these nanocomposite strain gages, and taking the time lag into account, there is still sometimes an issue with hysteresis. As can be seen in Figure 5-20, there is a slight difference in the loading vs. unloading portion of the cycle.

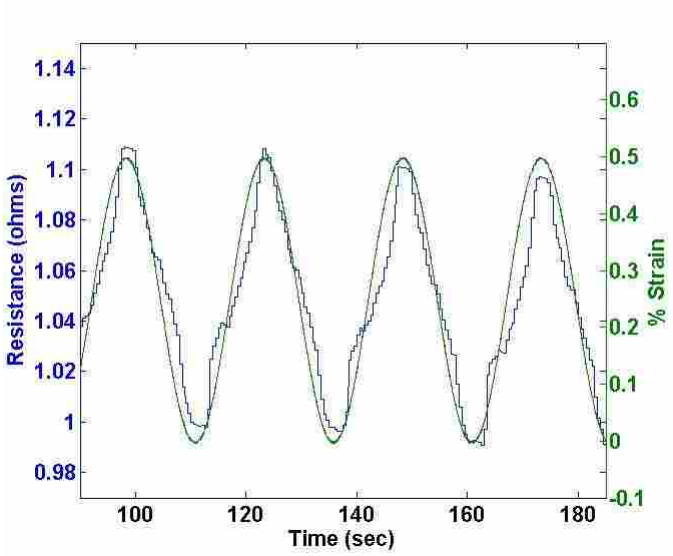

Figure 5-20: NiNs/Epoxy Nanocomposite Patch showing Hysteresis

To better visualize this hysteresis plots of resistance vs. strain are given in Figure 5-21 for cyclic frequencies of a) 0.04 Hz and b) 0.08 Hz. These two frequencies were tested in order to understand the reasons for this hysteresis. Because the hysteresis is larger for the lower frequency, it has been attributed to the viscoelasticity in either or both the carbon fiber composite and in the nanocomposite patches. This hysteresis can be taken into account in the calibration of the nanocomposite strain gage.

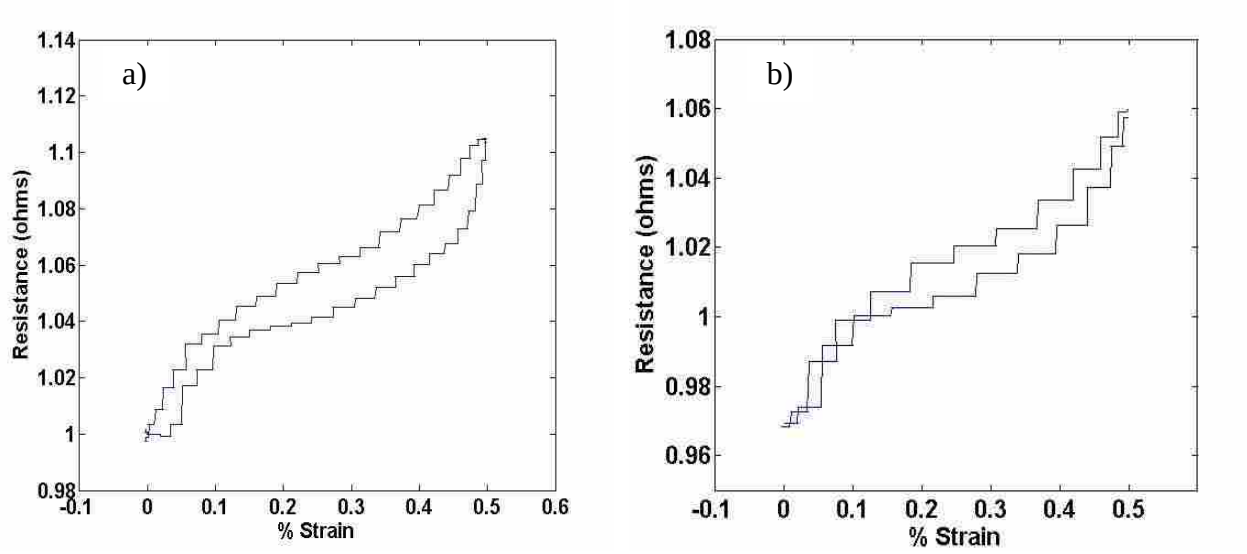

Figure 5-21: NiNs/Epoxy Strain Gage Hysteresis at Frequencies of a) 0.04Hz and b) 0.08 Hz

At even higher frequencies, such as 1 Hz, the hysteresis becomes indiscernible. This reduction in hysteresis is again attributed to the viscoelasticity, but at these higher frequencies the DAQ was collecting data in the high speed mode. In this mode, the level of noise could easily be too large to see any small amount of hysteresis still in the signal. To better investigate these smaller amounts of hysteresis, a noise filtering method may be needed in the high speed signal. A better DAQ could also be used which is capable of higher resolution.

By addressing the resolution, time lag, and hysteresis in the resistance signal, it ensures high quality strain measurement with these embedded nanocomposite strain gages. This high quality piezoresistive signal can now be calibrated to be used for in situ strain measurements in carbon fiber composites.

5.5 Calibration

The signal from any strain gage must always be calibrated in order to give a strain measurement. These embedded NiNs nanocomposite strain gages are no exception. A calibration was performed on the resistance signal from a representative NiNs/Epoxy nanocomposite bending sample. First, because a high resolution measurement was taken by the DAQ for this calibration, the half second time lag was removed from the data. Next, by performing a curve fit on the strain vs. resistance data (Figure 5-22(a)), a least squares approximation outputs an equation to calibrate the resistance signal into strain.

First a linear calibration, as shown in Figure 5-22(b), was performed followed by a third order polynomial fit displayed in Figure 5-22(c). It is clear that the nonlinear curve fit better followed the data, but due to the hysteresis, it is difficult to approximate the spread in the data. Therefore, two separate third order curve fitting calibrations were performed, one on the loading portion of the cycle and the other on the unloading portion. By taking the hysteresis into account the two separate curves better represented the relationship between strain and resistance as shown in Figure 5-22(d).

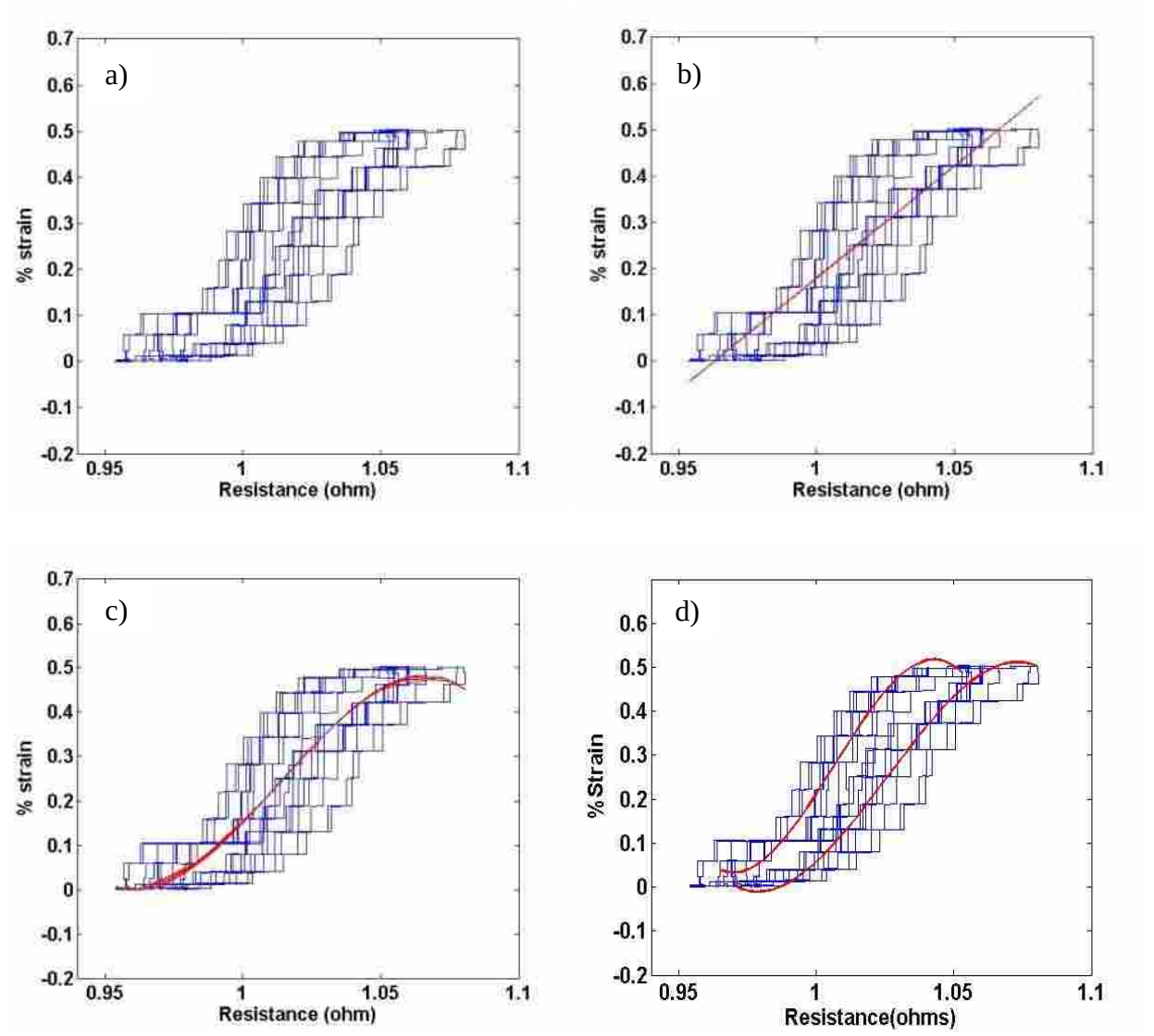

Figure 5-22: Strain verses Resistance with a) No Curve Fit, b) Linear Curve Fit, c) One Nonlinear Curve Fit and d) Separate Nonlinear Curve Fit for Up and Down for Hysteresis

The data before calibration is given in part (a) of Figure 5-23, with resistance on the left axis and strain on the right axis. The calibrated data is given in parts (b) through (d) of the same figure, displaying the calibrated strain from the nanocomposite strain gage on the left axis and the stain applied to the carbon fiber sample on the right axis. Figure 5-23(b) shows that the linearly calibration performs well. The nonlinear calibration also performs well, given in Figure

5-23(c), but does not appear to be significantly better than the linear calibration. Although the linear and nonlinear curve fits both provide reasonably accurate strain values, by taking the hysteresis into account a much more accurate calibration is attained as shown in Figure 5-23(d).

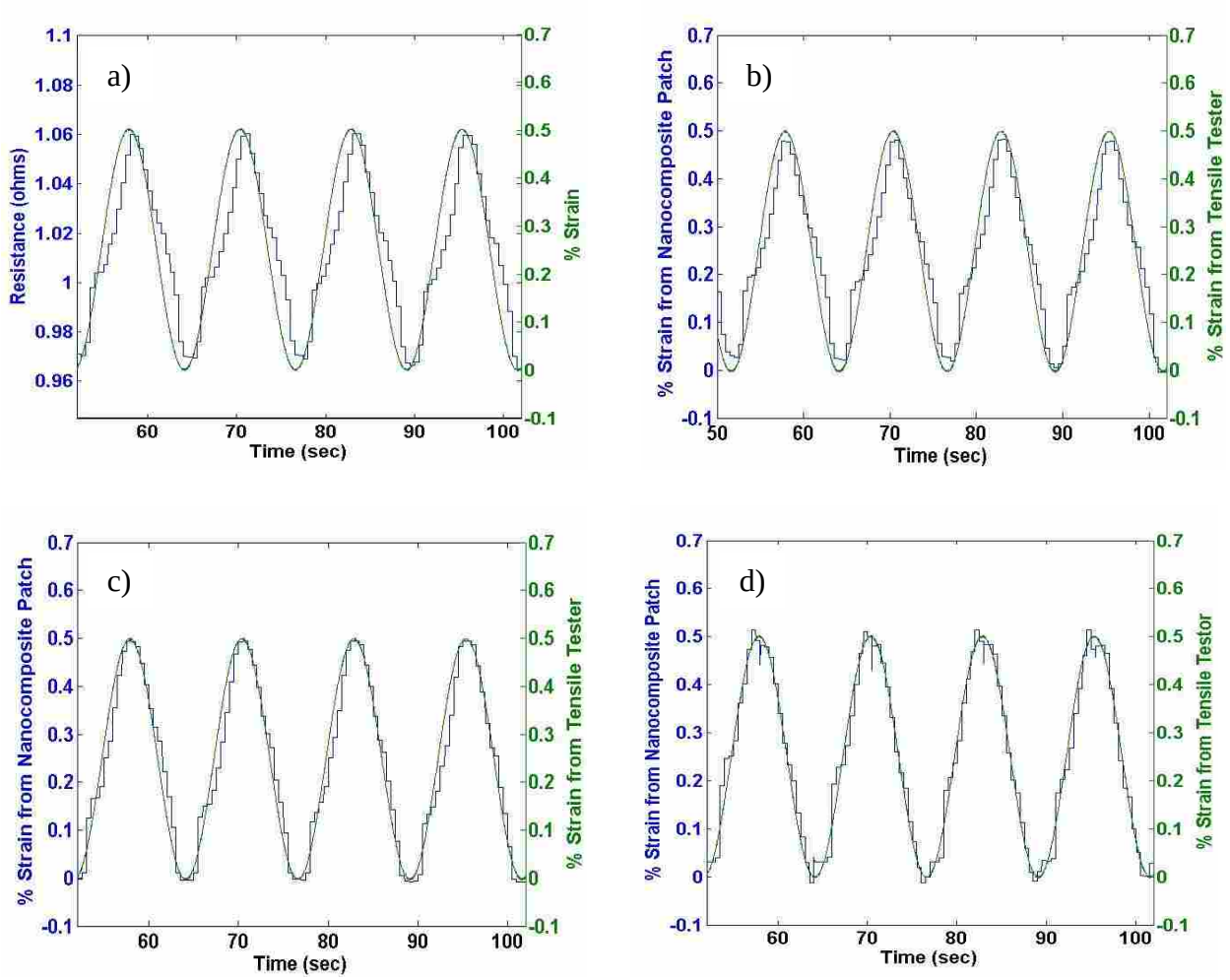

Figure 5-23: NiNs/Epoxy Patch with a) Data before Calibration, b) Linearly Calibrated Data, c) Nonlinearly Calibrated Data, and d) Separate Nonlinearly Calibrated Data for Hysteresis

5.6 Repeatability

To ensure accurate calibration for in situ strain measurement, repeatability is vital in the fabrication and embedding of nanocomposite strain gages. The fabrication processes are not

extremely well defined and the resulting gage properties are dependent on those processes. There are three ways that repeatability was investigated in this research. First is the signal repeatability over different strain frequencies, second is the repeatability between two different samples of the same type and third is the repeatability between strain cycles of the same sample.

With any strain measurement system it is hoped that the response will be repeatable for strain at any frequency. Tests were performed at several different frequencies on the same embedded NiNs nanocomposite strain gage for two different strain levels. The piezoresistive magnitude was measured for each frequency and the data was compiled into Figure 5-24. The figure shows that the signal is repeatable over the range of frequencies tested.

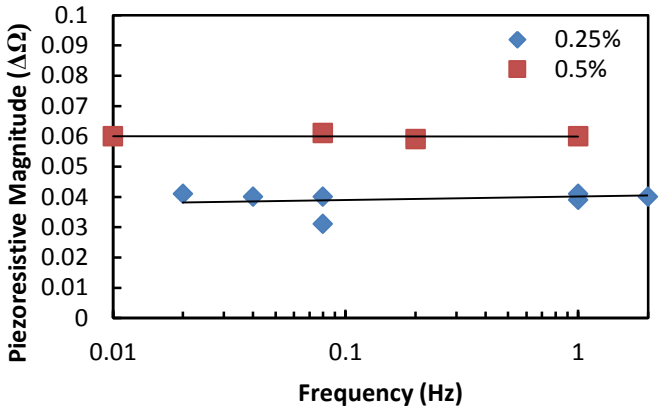

Figure 5-24: Graph showing no Strain Rate Dependency in NiNs Nanocomposite Gage

Next, the resistance signal from two NiNs/Epoxy type gages is given in Figure 5-25 showing repeatability between different samples of the same type. It can be seen that the signal profiles are very similar for both NiNs/Epoxy nanocomposite strain gages. The nominal resistance, and therefore the piezoresistive magnitude, is slightly different for these two gages, which is most likely due to the spacing of the wire electrodes in the sample. To obtain better

repeatability in resistance values from one gage to the next, a more consistent spacing should be defined.

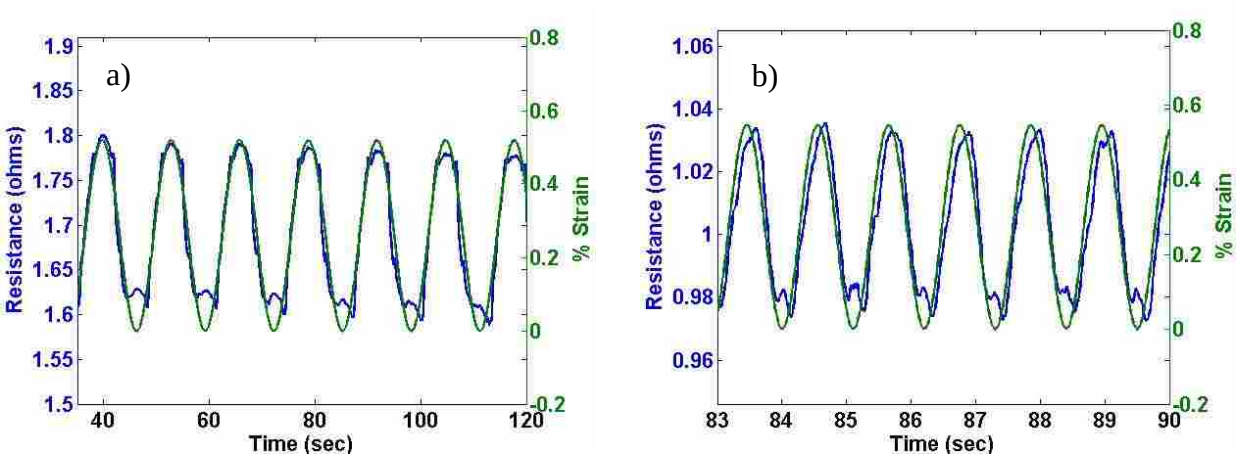

Figure 5-25: Two Different Epoxy Samples showing Repeatability in Signal

Finally, it is important that for different strain cycles of the same nanocomposite gage the piezoresistive signal is consistent. This is shown by Figure 5-26 which has a very repeatable signal measured for each of many cycles. The figure is displaying the last 30 of 1000 cycles all of which show similar repeatability. This demonstrates that the signal is repeatable for these types of embedded NiNs nanocomposite strain sensors.

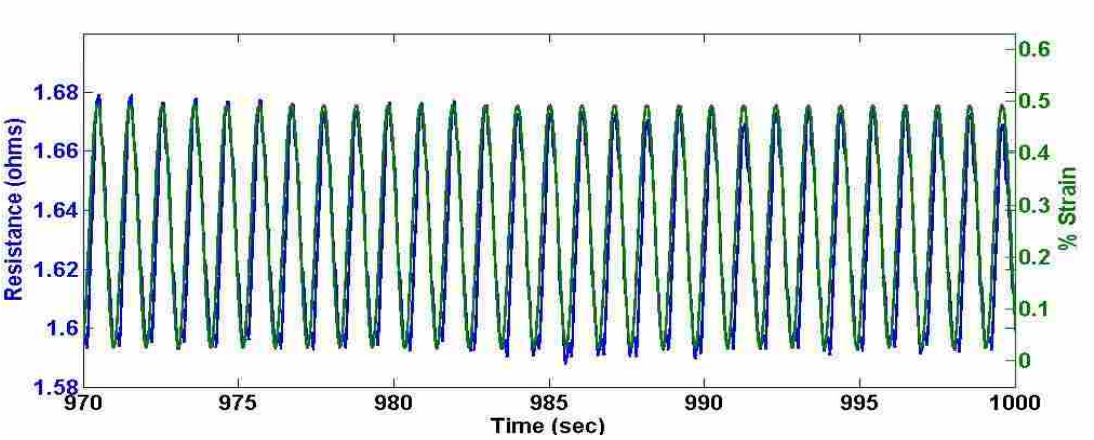

Figure 5-26: NiNs/Epoxy Patch showing Repeatability over 50 Cycles at 0.5% Strain

5.7 Nanocomposite Fatigue

Carbon fiber, due to its excellent fatigue characteristics, is often used in components which are to undergo high cycle loading. For a strain gage to be valuable in carbon fiber composite monitoring, the gage needs to last for many cycles as well. For one example, Figure 5-27 shows the resistance signal given by an embedded NiNs/Epoxy nanocomposite gage which had previously undergone nearly 5000 cycles.

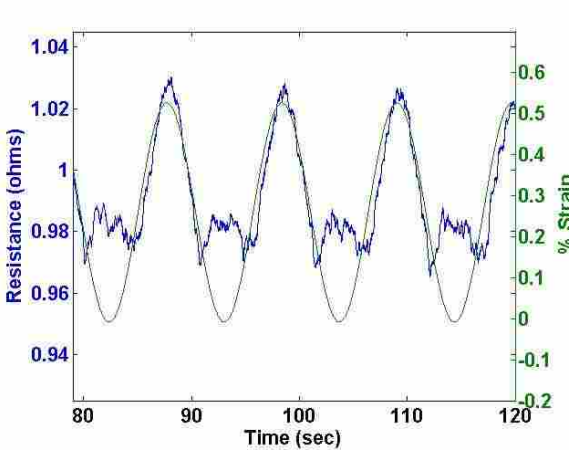

Figure 5-27: Strain Response after 4750 Cycles of NiNs/Epoxy Patch

Even after many thousand cycles the nanocomposite strain gage still shows its piezoresistivity. Due to testing constraints, hundreds of thousands of cycles were not performed, but this would be valuable for future work to determine if a fatigue limit existed for the nanocomposite patch.

Unlike the consistency in piezoresistivity for the NiNs/Epoxy nanocomposite gage, remember that the NiNs/Silicone nanocomposite gages show a rise in nominal resistance value over time (see Figure 5-13). The irreversible damage inflicted on this gage by many cycles means there will be a much shorter fatigue life than for the Epoxy type gage. Even after nearly 2000 cycles the nominal resistance value and piezoresistive magnitude did not stop rising.

Therefore, this type of strain gage seems to have a limited fatigue life. This could only be reliably used in a system where periodic calibration could verify the gage performance. How often calibration is required would depend on strain levels and cycle frequency.

5.8 Failure

Now that these NiNs nanocomposite strain gages have proven useful for in situ strain measurement of carbon fiber composites, the signal response during failure was investigated. Figure 5-28 shows an interesting phenomenon; at about 140 and 250 seconds there are slight shifts in the signal. These shifts were a result of a small amount of carbon fiber breaking. The audible snapping of these fibers occurred precisely when these shifts in signal were measured. A structural damage sensing system could trigger at this sort of shift in signal and notify users of fiber failure.

While it has been shown that these gages provide a good picture of the failure of small amounts of fiber, it is also of interest to see what happens in the measured resistance signal when the carbon fiber is completely failed. Figure 5-29 shows a NiNs/Epoxy nanocomposite strain gage signal as the sample was failed in a three point bend arrangement. As the strength of the carbon fiber composite is exceeded, the sample breaks in a brittle-like failure, as expected. The stress was calculated at the bottom surface of the sample, where the embedded patch is located, by the following equation for flexural stress in the three point bend arrangement. This equation is given as Equation 5-1.

$$\sigma_f = \frac{3PL}{2bd^2} \tag{5-1}$$

Where σ_f is the stress at the bottom surface, P is the force applied, d is the depth or thickness of the test sample, b is the width of the test sample and L is the distance between the lower supports.

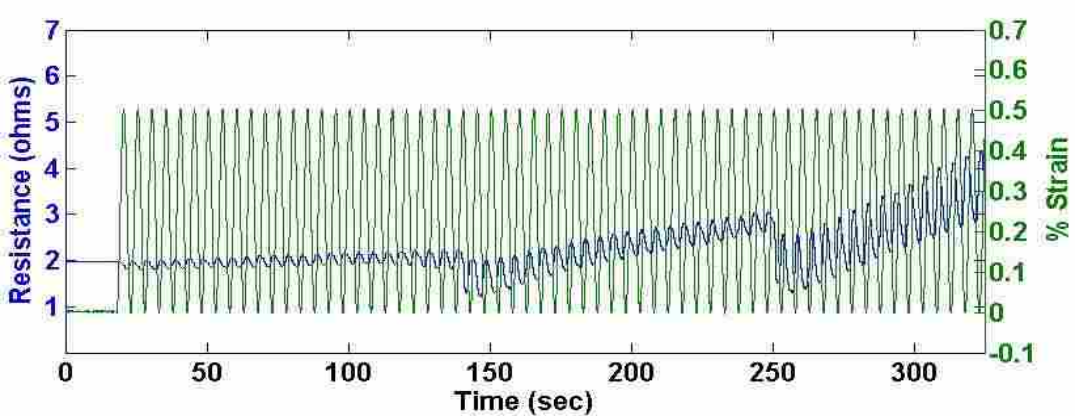

Figure 5-28: Graph showing some Carbon Fiber Breakage in Silicone/NiNs Patch

The signal not only accurately shows this failure with a large sharp spike in resistance at the precise time when the sample fails, but also shows a significant change in resistance preceding failure. This resistance change could be used to avoid failure by knowing the strain and stress in the sample as it approaches failure.

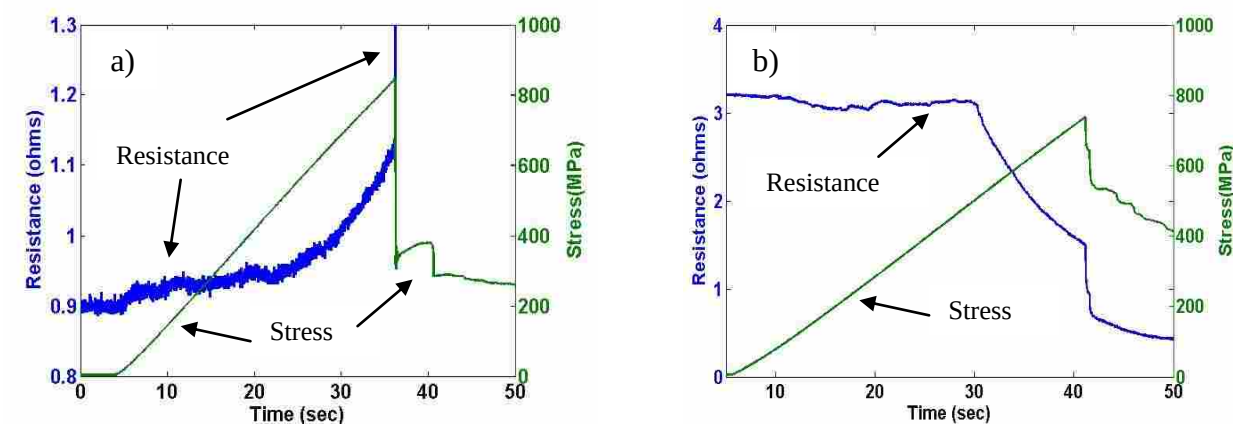

Figure 5-29: a) NiNs/ Epoxy and b) NiNs/Silicone Sample Types in Flexural Failure

The NiNs/Silicone nanocomposite patch shown in part (b) of the same figure also shows a sharp shift in resistance as the sample finally fails. However, it also shows a steep decrease in resistance which begins about 30 seconds into the test. This happens shortly after 0.5% strain, where most of the cyclic testing was performed; therefore the piezoresistive signals measured in the rest of the testing in this study will not reflect this dramatic change. Referring back to the work done by Oliver Johnson, this interesting phenomenon may be explained by the dramatic drop in resistance that he measured after the "knee" in the curve shown in Figure 2-4. This could prove to be a valuable trait for measuring strain levels closer to failure and warrants further investigation in future work.

A major concern with the introduction of any embedded sensor is the weakening of the carbon fiber composite in the vicinity of the sensor. To understand how these nanocomposite sensor types affect the material properties of the sample, the ultimate strength and elongation were measured for each failed sample type. Figure 5-30 is an example of one of the stress-strain curves used to get this data. All of the ultimate strength and elongation data was then compiled in Table 5-1.

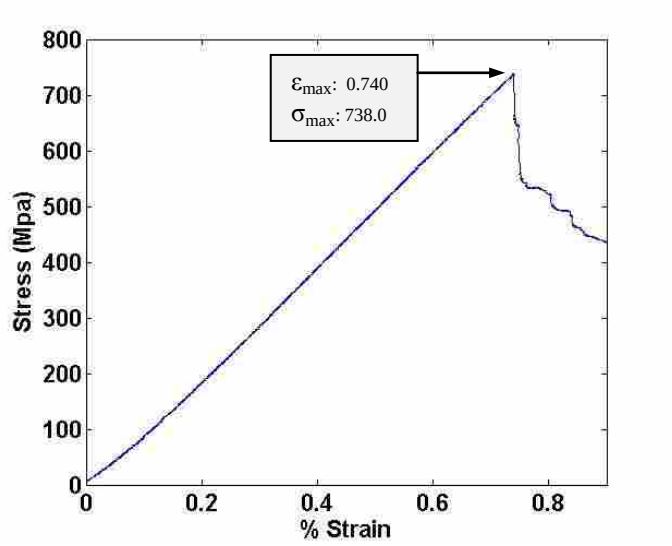

Figure 5-30: Stress-Strain Curve for NiNs/Silicone Sample

Table 5-1: Mechanical Properties at Failure

Sample Type	Ultimate Strength (MPa)	Standard Deviation (MPa)	Ultimate Elongation (%)	Standard Deviation (%)
Control Sample	898.9	146.9	0.656	0.148
Directly Embedded NiNs	589.5	211.9	0.603	0.034
Insulated NiNs/Epoxy	633.2	51.2	0.823	0.183
Insulated NiNs/Silicone	504.2	128.2	0.827	0.062

From the table we see that the directly embedded NiNs do in fact introduce a significant weakening of the composite along with the insulated nanocomposite samples. The directly embedded NiNs were not expected to introduce this level of weakening. However, the standard deviations are relatively high. Future testing could provide more consistent results. For the insulated samples the composite weakening could be reduced by using an insulating barrier thinner than the fiberglass, as well as by fabricating the nanocomposite patch as a thin film instead of casting it into the fiberglass compartment. The insulated samples reached a higher ultimate elongation which is most likely due to the lower Young's modulus in the fiberglass patch.

5.9 Applications

As a proof of concept for NiNs nanocomposite embedded strain sensors in carbon fiber composites, they were applied to two different applications. The first is the creation of a carbon fiber prosthetic foot with an embedded sensor for strain feedback. The second is a cylindrical tube of carbon fiber also fitted with embedded sensors. The cylindrical tube can be used to represent a segment of a pipe or circular beam under bending loads or a shaft undergoing torsion. These are specific, real world applications of carbon fiber composites. More detail on the prototype preparation and testing of these two applications will be given in this section. It is

important to remember that these are simple parts designed to prove the validity of the NiNs nanocomposite embedded sensor, but countless other applications in aerospace, aircraft, sporting goods, automotive and experimental testing are just as valuable.

5.9.1 Prosthetic Foot Prototype

Due to the high strength-to-weight ratios found in carbon fiber composites, as well as superior properties in fatigue, toughness, and corrosion resistance, it is an ideal material for the manufacture of prosthetics. As prosthetics get more advanced in their passive and active response to the movement of the wearer, it is important to get feedback from the prosthetic itself. One way to get this feedback would be the embedding of a NiNs nanocomposite strain gage. The level of strain, and therefore stress and load, can be invaluable feedback to the prosthetic controls.

Two different carbon fiber prosthetic foot prototypes were fabricated by a hand layup process using machining foam for the molding structure. After the machining foam was cut to the designed curvature and covered in a release film, layers of carbon fiber prepreg were placed on top in the desired layup pattern. The NiNs nanocomposite was then laid in between layers in the desired location as shown in Figure 5-31 and the remaining layers were placed on top. The prosthetic foot prototypes were then cured under vacuum in an autoclave. Figure 5-31(a) shows an everyday prosthetic foot prototype and (b) shows an athletic sprinters foot.

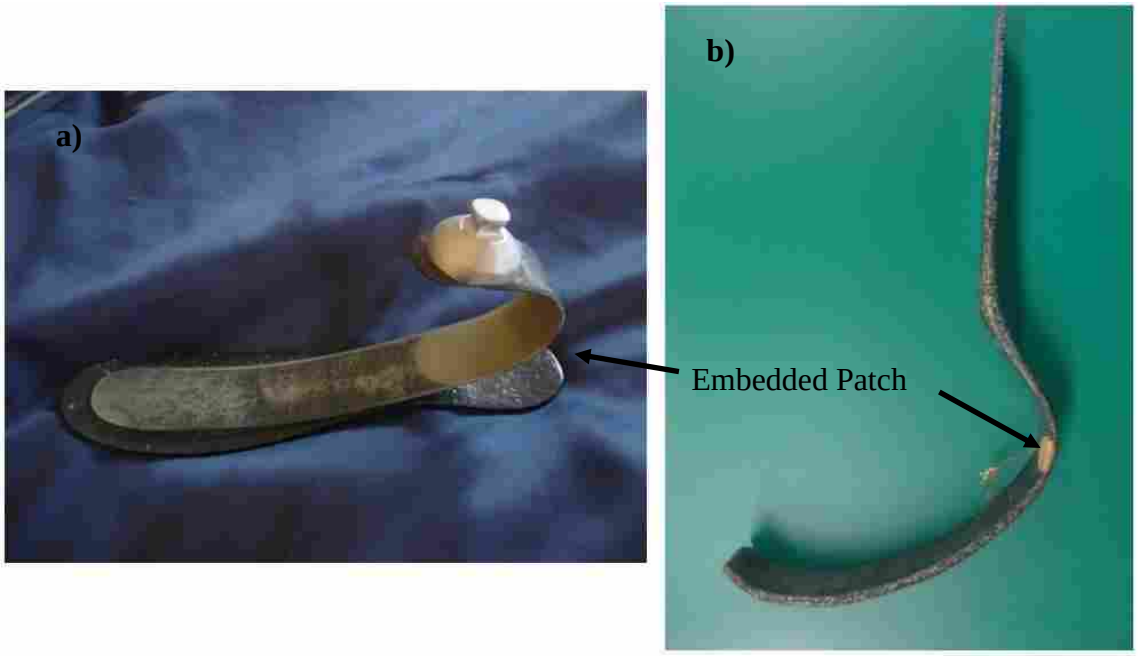

Figure 5-31: Two Different Prosthetic Foot Prototypes

A compressive load was applied by an MTS tensile tester to flex the "ankle" of the prosthetic. The resulting piezoresistive measurements from the embedded sensor in the sprinters foot is shown in Figure 5-32 with the sample undergoing several cycles.

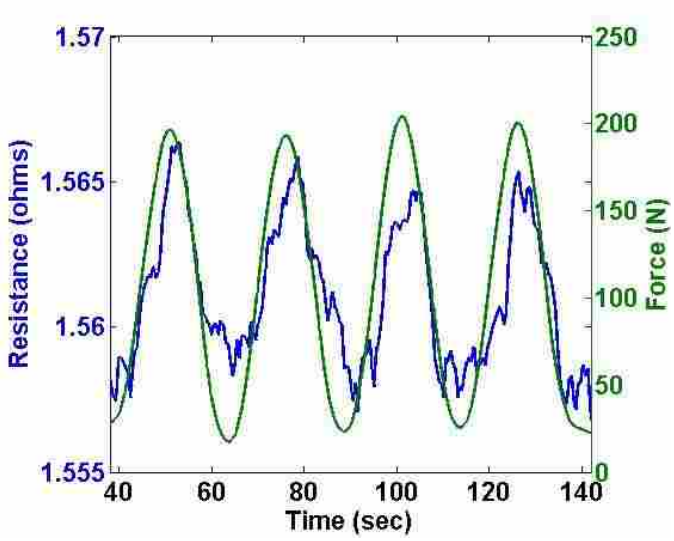

Figure 5-32: Prototype Prosthetic Foot with Embedded NiNs/Epoxy Strain Gage

It can be seen that the signal from the embedded patch is a reasonable representation of the loading cycle. Therefore, this prosthetic foot prototype shows that these nanocomposite strain sensors can be embedded in carbon fiber parts for real time in situ strain monitoring.

5.9.2 Cylindrical Tube

The weight reduction of cars, aircraft, spacecraft, and sporting goods is an increasingly important design requirement in these industries. To meet these demands the makers of these products are turning to the composite industry for many components such as beams, shafts, pressure vessels, etc. Many of these components experience large stresses and it would be valuable to measure that stress through embedded sensors. To show this concept a cylindrical tube was made, shown in Figure 5-33, to act as a beam, pipe, or shaft in either bending or torsion. This could also represent a golf club, fishing pole, bike frame, drive shaft or many other components in these industries.

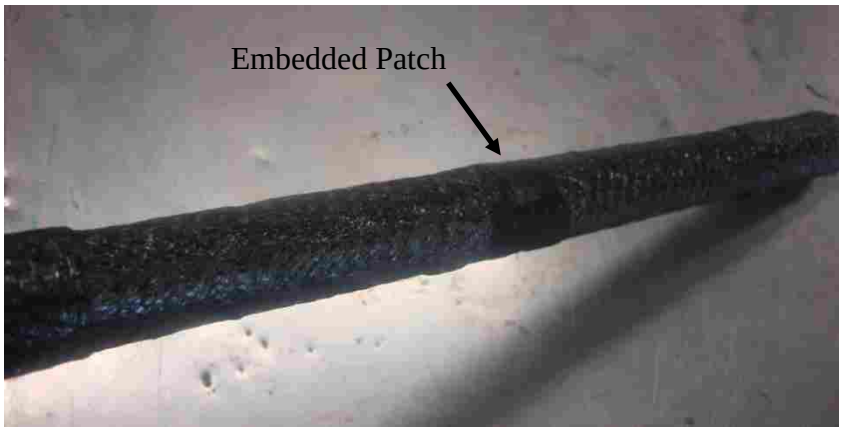

Figure 5-33: Carbon Fiber Cylindrical Tube

To construct this shaft a polished steel pipe was used as a mandrel. For ease of manufacture a carbon fiber fabric prepreg was roll-wrapped by hand onto the pipe. After rolling

the desired thickness of carbon fiber onto the mandrel, the embedded sensor was placed onto the shaft at the desired location and the remainder of the carbon fiber was rolled on. Release film and breather cloth were then applied and a shrink tape was tightly wound around it. When heated, this tape applies a radial compressive load throughout the curing process.

The three point bend test was performed causing the shaft to bend slightly; thus applying a tensile strain in the lower layers where the embedded sensor was placed. These results are given in Figure 5-34.

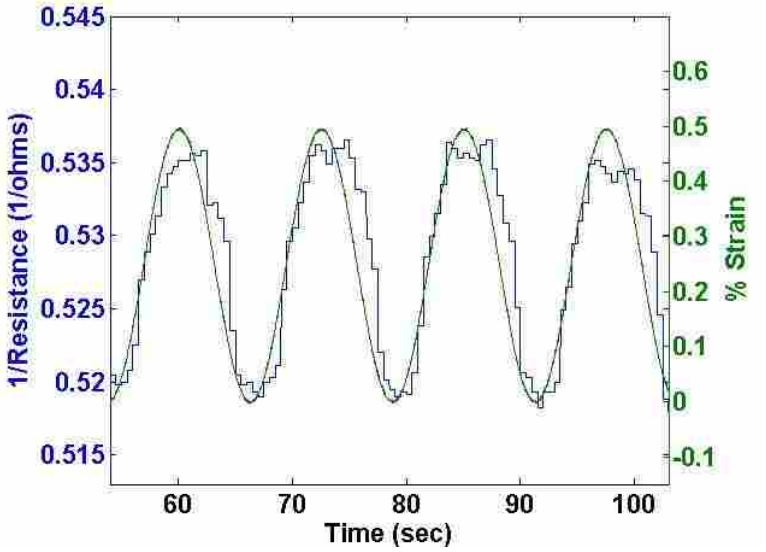

Figure 5-34: Cylindrical Tube with Embedded NiNs/Epoxy Strain Gage

Similar to the prosthetic foot, this prototype also shows that these embedded NiNs nanocomposite strain gages can be a powerful in situ strain monitoring tool in the carbon fiber industry.

6 CONCLUSIONS

A new and powerful technique has been presented for the measurement of strain in carbon fiber composites. This technique utilizes the piezoresistive properties of NiNs nanocomposites. Several methods of forming these nanocomposites have been shown to work and can be used real time and in situ. The directly embedded sample is the simplest method, but has the limitation of requiring unidirectional fibers and seems to significantly weaken the carbon fiber composite. The second method, insulating the nanocomposite strain sensor, can be used with any carbon fiber layup pattern, but also weakens the carbon fiber composite.

The method of placing the dry NiNs patch in between prepreg layers during the layup process is vastly easier than insulating the patch. It was shown that the piezoresistive signal is orders of magnitude greater than that which is reported from the carbon fibers themselves. On the other hand, due to the requirement of unidirectional fiber orientation, there are limitations to direct applications of this method.

The process of electrically insulating the nanocomposite patches can be used in more elaborate layup patterns for in situ strain measurements. The NiNs nanocomposite patches made with epoxy and silicone rubber both show significant resistance change when strained. However, due to the fatigue damage seen in the NiNs/Silicone gage type, the NiNs/Epoxy type sample has shown greater potential for industrial application as an embedded sensor.

This research is the first to investigate embedding NiNs nanocomposite strain gages into carbon fiber composites. Therefore, it was beyond the scope of this research to fully discover all the limitations and applications of this technology. The validity of these embedded NiNs strain gages in monitoring carbon fiber composites shown in this research demonstrates that it is worth investigating this technology in more detail.

For the large majority of carbon fiber composite applications, the insulated nanocomposite patches are the best option; specifically the NiNs/Epoxy type. This is due to several reasons. First, by using the insulated patches, any layup pattern can be used. Second, the insulated patch offers the potential for a higher piezoresistive magnitude because it is not limited by the overall resistance of the carbon fiber composite. Also, the NiNs/Epoxy type provided the most consistent signal for many cycles. While this gage does show good results, there is still a lot of future work that can be done.

Future work could include optimizing the piezoresistive response by varying how much NiNs is included in the insulated patch samples along with the potential to add chopped NCCF as was done by Oliver Johnson [36]. The polymer matrix in the nanocomposite can also be changed to increase piezoresistive response. This research has shown that different polymer matrix materials can have a large impact on the signal quality and gage life. Gaining a better understanding of why the NiNs/Silicone gages are breaking down (NiNs breakage or dislocation) would be helpful to improve signal quality. The dramatic drop in resistance measured prior to sample failure at strain levels above 0.5% for the silicone gages should also be investigated.

Significant weakening of the carbon fiber composites was shown in this research. The reasons this weakening occurs as well as the methods to overcome it should be investigated in future work. The nanocomposite size, thickness, and stiffness can be altered to lower this

weakening effect as well as the size and location of embedded wires. Different insulating materials besides fiberglass could be used to minimize overall patch size and thickness.

The overall fatigue limits of the embedded nanocomposite strain gages were not determined due to testing constraints. However, this would be valuable to investigate in the future. Another testing constraint was the limitation on strain rate that could be applied to the test samples. It would be valuable to know how fast these gages can measure strain.

This novel work has been presented at a SAMPE Utah Chapter seminar on the 10th of February 2011. A conference paper was also submitted, reviewed and accepted for the student research symposium at SAMPE Long Beach. This conference will include published conference proceedings, as well as a presentation to take place on May 24th, 2011 [43]. This work is also being submitted in April for publication with the Sensors and Actuators journal.

In conclusion, by embedding NiNs nanocomposite patches in between layers of carbon fiber composites, an accurate, repeatable strain measurement method has been created. Unlike other strain sensing methods, these embedded sensors are easy to employ and have the ability to measure strain real time and in situ. These strain measurement techniques enhance the ability to monitor fatigue in carbon fiber structures which will help to increase their safety and applications.

REFERENCES

[1] Bacon's breakthrough, in: National Historic Chemical Landmarks, American Chemical Society, 2007.

[2] Carbon fibers today, in: National Historic Chemical Landmarks, American Chemical Society, 2007.

[3] The Future of Carbon Fiber, in: Zoltek Carbon Fiber, Zoltek Corporation, 2010.

[4] A. Todoroki, Y. Samejima, Y. Hirano, R. Matsuzaki, Piezoresistivity of unidirectional carbon/epoxy composites for multiaxial loading, Composites Science and Technology, (2009) 1841-1846.

[5] T. Prasse, F. Michel, G. Mook, K. Schulte, W. Bauhofer, A comparative investigation of electrical resistance and acoustic emission during cyclic loading of CFRP laminates, Composites Science and Technology, (2001) 831-835.

[6] M.W. Hyer, Stress Analysis of Fiber-Reinforced Composite Materials, McGraw-Hill, Boston, 1998.

[7] M. Kupke, K. Schulte, R. Schuler, Non-destructive testing of the FRP by d.c. and a.c. electrical methods, Composites Science and Technology, (2001) 837-847.

[8] B. Tang, Fiber Reinforced Polymer Composites applications in USA DOT- federal highway administration, in: Korea/U.S.A Road Workshop Proceedings, 1997.

[9] N. Hu, Y. Karube, C. Yan, Z. Masuda, H. Fukunaga, Tunneling effect in a polymer/carbon nanotube nanocomposte strain sensor, Acta Materialia 56, (2008) 2929-2936.

[10] S. Wang, D.D.L. Chung, Negative piezoresistivity in continuous carbon fiber epoxy-matrix composite, Journal of Material Science, (2007) 4987-4995.

[11] L. Gao, E.T. Thostenson, Z. Zhang, T.-W. Chou, Coupled carbon nanotube network and acoustic emission monitoring for sensing of damage developement, Science Direct: Carbon, I (2009) 1381-1388.

[12] J.-M. Park, D.-S. Kim, S.-J. Kim, P.-G. Kim, D.-J. Yoon, K.L. DeVries, Inherent sensing and interfacial evaluation of carbon nanofiber and nanotube/epoxy composites using electrical resistance measurement and micromechanical technique, Science Direct-Composites Part B, B (2006) 847-861.

[13] J.-M. Park, P.-G. Kim, J.-H. Jang, Z. Wang, J.-W. Kim, W.-I. Lee, J.-G. Park, K.L. DeVries, Self-sensing and dispersive evaluation of single carbon fiber/carbon nanotube(CNT)-epoxy composites using electro-micromechanical technique and nondestructive acoustic emission, Composites: Part B, B (2008) 1170-1182.

[14] A.C. Iadicicco, Antonello; Cusano, Andrea;, Fiber Bragg Grating Sensors Advancements and Industrial Applications, Advances in Science and Technology, 55 (2008) 213-222.

[15] X. Zhao, J. Gou, G. Song, J. Ou, Strain monitoring in glass fiber rienforced composites embeded with carbon nanopaper sheet using Fiber Bragg Grating (FBG) sensors, Composites: Part B, (2009) 134-140.

[16] F.H. Gojny, M.H.G. Wichmann, U. Kopke, B. Fiedler, K. Schulte, Carbon nanotube-reinforced epoxy-composites: enhanced stiffness and fracture toughness as low nanotube content, Composites Science adn Technology, (2004) 2363-2371.

[17] S. Iijima, Helical microtubules of graphitic carbon, Nature, 354 (1991) 56-58.

[18] C.A. Cooper, D. Ravich, D. Lips, J. Mayer, H.D. Wagner, Distribution and alignment of carbon nanotubes and nanofibrils in a polymer matrix, Composites Science and Technology, (2002) 1105-1112.

[19] I. Kang, M.J. Schulz, J.H. Kim, V. Shanov, D. Shi, A cabon nanotube strain sensor for structural health monitoring, Smart Materials and Structures, (2006) 737-748.

[20] G.T. Pham, Y.-B. Park, Z. Liang, C. Zhang, B. Wang, Processing and modeling of conductive thermoplastic/ carbon nanotube films for strain sensing, Composites: Part B, (2008) 209-216.

[21] Materials Research Institute LLC, in: Products and Services, Beavercreek, OH.

[22] C.A. Martin, J.K.W. Sandler, M.S.P. Shaffer, M.-K. Schwarz, W. Bauhofer, K. Schulte, A.H. Windle, Formation of percolation networks in multi-wall carbon nanotube-epoxy composites, Composites Science and Technology, (2004) 2309-2316.

[23] H.D. Wagner, R.A. Vaia, Nanocomposites: issues at the interface, Materials Today, (2004) 38-42.

[24] G. Hansen, What we dreamt as children- How conductive polymers are bringing our dreams to reality, Journal of Advanced Materials, (2006) 68-74.

[25] J.-M. Park, S.-J. Kim, D.-J. Yoon, G. Hansen, K.L. DeVries, Self-sensing and interfacial evaluation of Ni nanowire/polymer composites using electro-micromechanical technique, Composites Science and Technology, (2007) 2121-2134.

[26] J.-M. Park, S.-J. Kim, J.-H. Jang, Z. Wang, P.-G. Kim, D.-J. Yoon, J. Kim, G. Hansen, K.L. DeVries, Actuation of electrochemical, electro-magnetic, and electro-active actuators for carbon nanofiber and Ni nanowire reinforced polymer composites, Composites: Part B, (2008) 1161-1169.

[27] O.K. Johnson, C.J. Gardner, N.A. Mara, A. Dattelbaum, G.C. Kaschner, T.A. Mason, D.T. Fullwood, B.L. Adams, G. Hansen, Multi-Scale Model for the Extreme Piezoresistivity in Silicone/Nickel Nanostrand Nanocomposites, in, 2008.

[28] O.K. Johnson, G.C. Kaschner, T.A. Mason, D.T. Fullwood, T. Hyatt, B.L. Adams, G. Hansen, Extreme piezoresistivity of silicone/nickel nanocomposites for high resolution large strain measurment, (2008).

[29] J. Sandler, M.S.P. Shaffer, T. Prasse, W. Bauhofer, K. Schulte, A.H. Windle, Developement of a dispersion process for carbon nanotubes in an epoxy matrix and the resulting electrical propeties, Polymer 40, (1999) 5967-5971.

[30] C.A. Martin, J.K.W. Sandler, A.H. Windle, M.-K. Schwarz, W. Bauhofer, K. Schulte, M.S.P. Shaffer, Electric field-induced aligned multi-wall carbon nanotube networks in epoxy composites, Plymer 46, (2005) 877-886.

[31] G. Hansen, N. Hansen, Conductive Composites Company, in: Conductive Composites Company, 2003.

[32] L. Liu, H.D. Wagner, Rubbery and glassy epoxy resins reinforced with carbon nanotubes, Composites Science and Technology, (2005) 1861-1868.

[33] E.Z. Meilikhov, Giant piezoresistivity of nanocomposites with the tunneling conductivity, Sensors and Actuators A: Physical, (2009) 187-190.

[34] X. Song, S. Liu, Z. Gan, Q. Lv, H. Cao, H. Yan, Controllable fabrication of carbon nanotube-polymer hybrid thin film for strain sensing, Microelectronic Engineering, (2009) 2330-2333.

[35] T. Yasuoka, Y. Shimamura, A. Todoroki, Electrical Resistance Change under Strain of CNF/Flexible-Epoxy Composite, Advanced Composite Materials, 19 (2010) 123-138.

[36] O.K. Johnson, Optimization of nickel nanocomposite for large strain sensing applications, Sensors and Actuators A: Physical, 166 (2010) 40-47.

[37] A.V. Kyrylyuk, P. van der Schoot, Continuum percolation of carbon nanotubes in polymeric and colloidal media, PNAS, (2007) 8221-8226.

[38] Four-terminal Sensing, in: Wikipedia, 2010.

[39] A.S.o.M. Engineers, ASME Standards, 2010.

[40] Voltage Divider, in: Wikipedia, 2010.

[41] J. Chan, Four-Point Probe Manual, in: EECS 143 Microfabrication Technology, 1994.

[42] T.R. Kuphaldt, Kelvin (4-wire) Resistance Measurment, in: All About Circuits, 2000.

[43] T.M. Johnson, D.T. Fullwood, G. Hansen, Strain Monitoring of Carbon Fiber Composite with Embedded Nickel Nanostrand Strain Gage in: SAMPE, Long Beach, CA, 2011.

[44] N. Lachman, H.D. Wagner, Correlation between interfacial molecular structure and mechanics in CNT/ epoxy nano-composites, Composites: Part A, (2009) 1093-1098.

[45] J.K.W. Sandler, S. Pegel, M. Cadek, F. Gojny, M. van Es, J. Lohmar, W.J. Blau, K. Schulte, A.H. Windle, M.S.P. Shaffer, A comparative study of melt spun polyamide-12 fibers reinforced with carbon nanotubes and nanofibers, Polymer 45, (2004) 2001-2015.

[46] Q. Zhao, M.D. Frogley, H.D. Wagner, Direction-sensitive strain-mapping with carbon nanotube sensors, Composites Science and Technology, (2002) 147-150.

[47] O. Becker, R.J. Varley, G.P. Simon, Use of layered silicates to supplementarily toughen high performance epoxy-carbon fiber composites, Journal of Material Science Letters, (2003) 1411-1414.

[48] E.J. Garcia, B.L. Wardle, A.J. Hart, Joining prepreg composite interfaces with aligned carbon nanotubes, Composites: Part A, (2008) 1065-1070.

[49] Q. Zhao, M.D. Frogley, H.D. Wagner, The use of carbon nanotubes to sense matrix stresses around a single glass fiber, Composites Science and Technology, (2001) 2139-2143.

APPENDIX A. DISPERSION METHODS

The dispersion of nanoparticles into a polymer matrix is the biggest issue in manufacturing nanocomposites. When these particles are not uniformly distributed they can introduce many issues, both electrical [37] and mechanical [19]. For instance, it has been reported that if CNT are not dispersed evenly the polymer will show similar mechanical properties to that of a major defect in the microstructure [13, 44]. In a similar vein, the electrical properties will also be grossly distorted by poor distribution. Several dispersion methods have been verified including ultrasonic mixing, calendaring, Dremel tool, dry mixing and planetary centrifugal mixing (THINKY®). These methods will be discussed here in some detail.

A.1 Ultrasonic

The most common technique used for the distribution of nanoparticles is the ultrasonic mixing of the particles into the matrix [13, 16, 34, 44]. The ultrasonic frequencies and intensities used result in very large sheer forces which separate and distribute the particles. This method usually involves two main features: first, the use of a solvent and second, a long time to mix. When the nanoparticles are put into a solvent the ultrasonic mixing is much more effective. The solvents used were standard solvents like ethanol, acetone, 2-propanol, etc. with acetone and 2-propenol shown to be most effective. The ultrasonic mixing also requires large amounts of time to mix. For a few examples: Pham reports 2 hrs of mixing [20], Lachman used 3 or more hrs

[44], Park reported 12 hrs [13], and Kang reported up to 20 hrs [19]. These high sheer forces are perfect for the mixing of tough particles like CNTs, but will break the brittle NiNs structure. Therefore this method is predominantly used on CNTs. The large amount of time needed to mix and the small batch sizes that can be mixed at one time have lead researchers to investigate other mixing methods that are more easily scaled up.

A.2 Calandaring (Rollers)

To speed up the mixing of CNTs into a polymer base, Gojny and Gao have employed another high sheer mixing method called calendaring. This method employs ceramic cylinders with very small gap size between them. The rolls are turned at different rates and the resultant shear forces act to mix the CNT into the polymer evenly. Both Gojny and Gao used a three roller calendaring method [11, 16]. The gap size is on the order of 5 micrometers, with roller rates from 20-180rpm [16]. This is a much easier method to scale up for large batches, but once again this is a high sheer method and will not work for NiNs.

A.3 Dremel Tool

An interesting method reported by Kang in the Smart Materials Nanotechnology Laboratory in Cincinnati, Ohio was the simple use of a high speed Dremel drill. While this method proved effective in CNT distribution, it still had to mix for 4 hrs at an elevated temperature [19]. This method may be easier without more expensive equipment, but still required significant amounts of time for a small batch size, i.e. it too is hard to scale up for larger production. This method had not been tried with NiNs.

A.4 Dry Mixing Methods

Another method that has been employed by researchers is the method of mechanically mixing small solid particles of polymer in with the CNTs. As the conglomeration is mixed the CNTs tend to evenly distribute themselves onto the surface of the polymer particles. This type of mixing is generally used when there is going to be a mechanical extrusion, or compression method to create the samples. These methods use the pressure of the extrusion or compression process itself to melt the polymer and help to distribute the particles further. In the case of Cooper, they first ultrasonically mixed in a solvent and then dried the particles for more mixing and the extruding process they used [18]. Sandler, on the other hand, placed the CNT and polymer pellets directly into a micro-extruder, but the extrusion process was not the entire mixing method. After extrusion the fiber, about 1mm in diameter, was then put into a capillary rhoemeter which spins the fiber down to a diameter of approximately 125 micrometers. These fibers showed good CNT uniformity [45]. In another research group Pham put the polymer into a blender with a 75g pulverizer cup for about 2hrs and later added MWCNTs and blendered again for a couple of minutes for mixing. After this dry mixing method the powder was hot pressed with a 10-ton hydraulic press. The thin sheet that resulted was cut into several pieces, stacked up, and pressed again to ensure uniform distribution of the MWCNTs [20]. This method will not work in this research because the sample preparation methods are different than the ones used here.

A.5 THINKY®

The previous methods have employed very high sheer forces and sometimes considerable amounts of time. As mentioned this works well for CNTs which are so strong and uniform. On the other hand the brittle NiNs need more gentle mixing methods [25]. The technique that has

been employed by Johnson is the use of a THINKY® planetary centrifugal mixer [28]. The NiNs are mixed by hand into the polymer base and then placed into the THINKY®. The mixture is then spun to very high centrifugal forces. In opposition to the mixing of CNTs, this technique only works with very short amounts of mixing, on the order of 15-30 seconds. Screening the mixture also helps to break up large clumps of NiNs [28]. This was the method used in this research.

APPENDIX B. FIBER ORIENTATION AND HYBRID COMPOSITES

A few topics also covered in the literature review, but which were not included in this thesis are fiber orientation, and the limited research on hybrid composites. These topics will be discussed here.

B.1 Fiber Orientation

At times the orientation of the nanofibers is important to the properties or desired applications of the nanocomposite. There are many reasons that the fibers would need to be aligned and several methods for aligning them. In the case of CNTs, the reasons for aligning the fibers are mostly mechanical [18, 25]. It has been reported by Martin that the aligning of CNTs did not help to increase the electrical network [30]. Zhao aligned the CNTs for Raman band measurement. In order for this measurement method to show stresses in certain directions, the fibers either need to be aligned or a polarization lenses can be used on the sensor [46].

With the different reasons to align the nanofibers in the polymer, researchers have found several methods that work well for aligning them. The application of electrical or magnetic fields during the curing process is the most common way. Both AC and DC electric fields have been shown to work to some degree, with AC being more effective [30]. Another effective means for aligning fibers, specifically NiNs, is the use of a magnetic field. This was shown by Park to align the NiNs much more easily than the aligning of CNTs [25]. Nanoparticles can also be aligned

through mechanical methods as well. An extrusion based process has shown to align CNTs [18]. This can result in a greater mechanical reinforcement in one direction than the other.

B.2 Combining Nanocomposites with Carbon Fiber Composites

While the uses and properties of nanocomposites and fiber reinforced polymers have been examined separately from one another, this section will show how scientists are pushing the limits of material science and creating hybrid composites utilizing the best qualities of both fields. These hybrid composites are opening up huge opportunities for the creation of smart materials that will change the world of science and engineering. Several brief sections will outline the most pertinent research on these hybrid composites. This will include the use of nanoparticles to reinforce mechanical and electrical properties of carbon and glass fiber composites, experimental methods to understand the interactions of these two fields, composite fibers, and strain sensing in glass fiber composites by dispersion of CNTs. The exploration into these hybrid composites is very limited at this time. The possibilities have not yet been fully realized. Although the research reviewed here does not directly apply to the research in this thesis, it is very similar and therefore, was included here.

B.2.1 Strengthening of Advanced Composites with Nanoparticles

In a paper by Becker [47], the mechanical properties of high strength carbon fiber composites were enhanced by the introduction of nanoparticles into the matrix material. In traditional carbon fiber composites there is an issue with toughness in the translaminar direction. Separate layers of prepreg are laid up and the matrix holding the fibers together will tend to fail before the fibers themselves. In order to strengthen composites in this direction many techniques have been employed; these include the use of 3D pre-forms, interlaminar stitching, or composite

knitting. These techniques are often not as effective as desired. To combat this weakness Becker was incorporating nanoparticles interlaminarly to toughen the carbon fiber composite. The results of this type of reinforcement are very impressive, with fracture energy being increased by several times the original [47]. A similar result was found by Garcia [48] and his group when they placed a "forest" of CNTs in between prepreg layers of carbon fiber. These CNTs were rolled into the surface of the prepreg directly off of the silicon substrate they were grown on. Subsequently, the layer could be placed onto another prepreg sheet and cured as usual. This group also had great success with increases of 2.5 to 3 times the initial toughness [48].

B.2.2 Single Carbon Fiber in Nanocomposite Epoxy w/Fibers

A unique method for testing the interaction of nanofibers and standard fibers was employed by Park and his group. Their unique electro-micromechanical technique utilized a single carbon fiber embedded into a nanocomposite. The group performed many tests with both CNTs [13] and NiNs [25] nanocomposites. This research shows an accurate strain measurement technique through the electrical measurement methods they employed. These measurements were taken through the macro carbon fiber and it shows that the nanoparticles formed an effective electrical network also utilizing the conductivity of the carbon fiber [12].

B.2.3 Strain Sensing in Glass Composites

Strain sensing in glass reinforced composites has also benefited from the use of nanoparticles. Unlike carbon fibers, glass fibers are not active for Raman wave-number sensing and are not piezoresistive. This would eliminate most inherent strain monitoring methods all together without the introduction of CNTs into the composite. Even at low CNT content, stresses in the polymer matrix were easily measured with Raman sensing [49]. Another research group

lead by Gao introduced enough CNTs into the glass fiber matrix to create a conductive glass composite. This hybrid composite was able to sense strain and damage in itself [11]. Acoustic emission was concurrently employed to better understand the damage propagation.

In conclusion, it can be seen that although researchers have extensively studied the properties of nanocomposites and carbon reinforced composites, the combining of the two technologies has only been touched on. This leaves much room to investigate the possibilities of accurately and simply measuring strain in carbon fiber composites through the use of nanocomposite strain gages.